National Research University Higher School of Economics

As a manuscript

Alexey O. Kazakov

PSEUDOHYPERBOLIC ATTRACTORS AND MIXED DYNAMICS IN MULTIDIMENSIONAL DYNAMICAL SYSTEMS

DISSERTATION SUMMARY
for the purpose of obtaining academic degree
Doctor of Science in Applied Mathematics

Moscow
2021

The dissertation work was carried out at the National Research University Higher School of Economics.

Scientific consultant: Sergey Gonchenko, Doctor of Physical and Mathematical Sciences, Leading Research Fellow of the Institute of Information Technologies of Mathematics and Mechanics, Lobachevsky State University of Nizhny Novgorod.

1 Introduction

Relevance. Nowadays, the theory of dynamical chaos is a rapidly developing branch of the exact sciences. The creation of new methods of mathematical modeling and studying chaotic dynamics is one of the most urgent problems in this area. It is worth noting that over the past decades, chaotic dynamics of low-dimensional systems (three-dimensional systems of differential equations and two-dimensional maps) has been studied quite well, while the theory of multidimensional chaos is still far from to be completed.

In this dissertation work, new qualitative and numerical methods for the analysis of multidimensional chaotic dynamics, based on the theory of pseudohyperbolic attractors and the theory of mixed dynamics are proposed. Both of these theories arose quite recently, thanks to the works by Gonchenko, Turaev, Shilnikov, Newhouse, and were allowed to take a fresh look at a number of problems of a multidimensional chaos.

Among such problems, the following two problems can be distinguished: (1) do there exist "genuine" strange attractors other than hyperbolic and singular-hyperbolic (Lorenz) attractors; (2) how to explain the phenomenon of visual overlapping a chaotic attractor and a chaotic repeller, which is often observed in numerical experiments. The second problem is closely related to such important questions of the theory of dynamical systems as, for example: can hyperchaos arise in systems of low dimension and how to prove the absence of a smooth invariant measure in chaotic reversible systems. In the works of the dissertation applicant, answers to these questions were obtained using the above theories. In particular, examples of genuine (pseudohyperbolic) attractors were given for both four-dimensional systems of differential equations and three-dimensional diffeomorphisms. The application of the concept of mixed dynamics allowed the dissertation applicant to answer positively the question of the appearance of hyperchaos in two-dimensional diffeomorphisms, and also to establish the absence of a smooth invariant measure in the well-known problem of V.V. Kozlov on the motion a disk on a rough plane.

Thus, both theories of pseudohyperbolic attractors and mixed dynamics, turned out to be very efficient in solving applied problems. Qualitative and numerical methods developed in the dissertation work were used by the applicant to study models of nonholonomic mechanics, hydrodynamics, theory of coupled oscillators, as well as some other problems of nonlinear dynamics. It is worth noting that these methods can be applied to a wider class of problems. As a result of the dissertation work a number of new dynamic phenomena were discovered: the phenomenon of instant appearance of mixed dynamics, as a result of the collision of an attractor and a repeller; strongly dissipative mixed dynamics (when the numerically observed chaotic attractor and chaotic repeller intersect, but differ significantly, although theoretically they should almost coincide); new examples of pseudohyperbolic attractors were found: a wild spiral attractor in a four-dimensional system of differential equations, a figure-eight attractor in

the nonholonomic model of Chaplygin top, a discrete heteroclinic attractor in three-dimensional Hénon map, etc; new types of reverse in nonholonomic dynamics of a rigid body – for spherical bodies with the displaced center of mass.

It is important to note that problem (1) is closely related to one of the most important and difficult problems of the theory of dynamical systems: how to distinguish "genuine" strange attractors from the so-called quasiattractors, which, although demonstrate chaotic behavior of trajectories, but only on the physical level of rigor. Quasiattractors (according to Afraimovich and Shilnikov) either contain stable periodic orbits (with absorbing domains that may not be detected in numerical experiment), or such orbits appear under arbitrarily small perturbations. Thus, when studying a quasiattractor, it is impossible to distinguish chaotic dynamics from a long transient process, after which the trajectories will tend to a regular regime (stable periodic orbit). Genuine strange attractors (for example, such as hyperbolic attractors, Lorenz attractors, etc.) have the property that each their orbit has a maximal positive Lyapunov exponent, and this property persists for all close systems. Thus, chaotic dynamics demonstrated by systems with such attractors is persistent with respect to small perturbations. In contrast, quasiattractors are characterized by the presence of the so-called stability windows – regions of parameter values in which the attractor is simple, for example, a limit cycle.

Until recently, only hyperbolic and Lorenz attractors could be classified as genuine chaotic attractors. The situation drastically changed after the discovery of wild pseudohyperbolic attractors by Turaev and Shilnikov in 1998. Such attractors, in contrast to hyperbolic and Lorenz ones, admit homoclinic tangencies and, as a result, contain wild hyperbolic sets of Newhouse, which indicates the fundamental impossibility of a complete description of their dynamics and bifurcations. Nevertheless, stable periodic orbits do not appear inside such attractors due to the main property of pseudohyperbolicity, which ensures exponential expansion of volumes in some subspaces of the tangent space. This automatically implies that any trajectory of the attractor has a positive maximal Lyapunov exponent. Thus, the study of strange attractors with the pseudohyperbolic structure is fundamentally important from the applied point of view, since, having established the pseudohyperbolicity of the attractor, the researcher can be sure that this type of chaotic behavior is not destroyed with small changes in the parameter values of the system. The problem of developing the theory of pseudohyperbolic attractors occupies one of the central places in the dissertation work.

In this direction, new efficient methods were developed for checking the pseudohyperbolicity conditions of attractors of both systems of differential equations and diffeomorphisms. These methods are based on the direct verification of all conditions from the definition of pseudohyperbolicity. It should be emphasized that if at least one of these conditions is not fulfilled, then the attractor is not pseudohyperbolic and, according to the PQ-hypothesis (pseudohyperbolic or quasiattractor), suggested by the dissertation applicant, it must be a quasiattractor. The fulfillment of all the pseudohyperbolicity conditions allows one to conclude that the observed attractor is a genuinely chaotic attractor. In the works of the dissertation applicant, the numerical implementation of the developed method has shown its effectiveness on the example of a number of attractors in systems from various applications.

To solve problem (2), the concept of mixed dynamics was applied in the dissertation work. Mixed dynamics is the third form of dynamical chaos, the discovery of which refers to one of the recent achievements of theory of dynamical systems. Before the discovery of mixed

dynamics, it was traditionally believed that chaos in dynamical systems occurs only in two completely different forms: conservative chaos, typical, in particular, to Hamiltonian systems; and dissipative chaos, the mathematical image of which is a strange attractor – a nontrivial closed invariant set to which all orbits from its neighborhood tend. In the works of Gonchenko, Turaev, and Shilnikov, it was shown that a strange attractor can intersect with a strange repeller (an attractor of a system in backward time) along a closed invariant set, the so-called reversible core, which attracts nothing and repels nothing. This, of course, is a fundamentally new, third, form of chaotic behavior of orbits, which combines both dissipative (attractor / repeller) and conservative (reversible core) elements of dynamics.

The first specific examples of systems from applications that explicitly demonstrate this new type of dynamical chaos were found in the works of the dissertation applicant. In particular, the presence of mixed dynamics was shown in a number of problems of nonholonomic mechanics, in chains of coupled oscillators, as well as in problems of vortex dynamics. The discovery of mixed dynamics in models from applications led to the need to create a theory, which, in particular:

- allows one to explain the intersection of the chaotic attractor and the chaotic repeller observed in numerical experiments;
- explains which mechanisms (bifurcation scenarios) can result in mixed dynamics.

The second part of series of papers presented in the dissertation work is devoted to the solution of these problems, as well as to the description of various types of mixed dynamics phenomenon, and its applications to the study of specific systems.

As part of the dissertation work, a number of new numerical methods was developed. These methods make it possible to check the pseudohyperbolicity of strange attractors, to identify region corresponding to each of the three types of dynamical chaos in the parameter space, to construct diagrams of homoclinic bifurcations with minimal computational costs, etc. The developed methods were are implemented in the framework of software package "Computer dynamics: Chaos" (patents RU 2014619001 and RU 2016660109), a brief description of which is given in the third part of the dissertation work.

State-of-the-art.

Pseudohyperbolic attractors. Until recently, only hyperbolic and singular-hyperbolic (Lorenz) attractors could be classified as genuine strange attractors of smooth dynamical systems. The foundations of theory of hyperbolic attractors were laid in the 60s in the classical works of Anosov, Bowen, Williams, Mané, Pugh, Robinson, Sinai, Smale, Shilnikov, etc. At present, this topic continues to remain very relevant, both in the direction of the development of hyperbolic attractors theory, where significant results were obtained in the works of Aronson, Grines, Zhuzhoma, Medvedev, Pochinka, etc., and in the field of applications of this theory. Note that hyperbolic attractors were not known in applications for a long time. The situation changed after the papers by S.P. Kuznetsov, where such attractors were found in various physical models. The first such attractor appeared in his work in 2005, and now, thanks to the works of Kuznetsov, Kuptsov, I. Sataev, and others, a number of physical systems with hyperbolic attractors are known.

Unlike hyperbolic, singular-hyperbolic attractors are not structurally stable. Despite the fact that the first example of such an attractor was given in the work of E. Lorenz in 1963,

for a long time this work was not known to mathematicians. Only at the end of the 70s, several papers devoted to the mathematical theory of the Lorenz attractor appeared at once. Among them, the most significant are the well-known works of Afraimovich-Bykov-Shilnikov, Gukenheimer-Williams, and Bunimovich-Sinai. Later, in the works of Morales, Pacifico, Pujals, and E. Sataev, the theory of singular-hyperbolic attractors was developed, which, in a sense, generalized the theory of the Lorenz attractors.

As is now known, hyperbolic and singular-hyperbolic attractors form only a certain subclass of the set of pseudohyperbolic attractors. Among the latter, a special place have wild pseudohyperbolic attractors, the mathematical theory of which was laid down in the works of Turaev and Shilnikov. Systems with such attractors, in contrast to systems with hyperbolic and singular-hyperbolic attractors, admit homoclinic tangencies. However, bifurcations of these tangencies do not lead to the emergence of stable periodic orbits, due to the presence of a pseudohyperbolic structure, which ensures the existence of two transverse subspaces, strongly-contracting and central-unstable. Volumes in the central-unstable subspace are expanded. We also note that Turaev and Shilnikov (in 1998) proposed a phenomenological model of the wild spiral attractor of a four-dimensional system containing a saddle-focus equilibrium state. The first and so far the only example of such a model – in the form of a specific system of four differential equations – was constructed quite recently in one of the papers of the dissertation applicant.

One more principally important result in the theory of pseudohyperbolic attractors was obtained in the paper by Gonchenko, Ovsyannikov, Turaev, and Simo (2005), in which the existence of a discrete pseudohyperbolic analog of the Lorenz attractor was established for three-dimensional diffeomorphisms. In this work, it was also shown that pseudohyperbolic attractors, in contrast to hyperbolic ones, can appear in models of a very different nature, from which too many restrictive conditions are not required. Thus, the problem of finding such attractors and checking the conditions for their pseudohyperbolicity becomes very urgent. If situation are more or less good with the first part of this problem – a number of such attractors were found in the works of A. Gonchenko, S. Gonchenko, Ovsyannikov, Turaev, and others – the second part of this problem was far from the solution for a long time. The known methods based on the analysis of only the spectrum of Lyapunov exponents do not allow to obtain completely convincing results here. A universal approach that allows to verify all the conditions from the definition of pseudohyperbolicity of strange attractors for a fairly wide class of dynamical systems was developed within the framework of this dissertation work.

However, particular cases of pseudohyperbolicity (uniform hyperbolicity and singular hyperbolicity) for some specific systems have been verified earlier. Among the corresponding studies, it is important to note the works of S.P. Kuznetsov, Kuptsov, Tucker, Zgliczyński, Capiński. In particular, in the famous paper by Tucker (1999), the singular hyperbolicity of the classical Lorenz attractor was established by means of computer-assisted proof methods and, thus, the well-known Smale problem was solved. In the works of S.P. Kuznetsov and Kuptsov effective methods for checking the absence of tangencies between contracting and expanding subspaces, which is one of the necessary conditions for hyperbolicity, was proposed. In their paper in 2018, these methods were modified for the verification of the absence of tangencies between the contracting and central-unstable subspaces in the case of pseudohyperbolic attractors. In the work of Capiński, Turaev, and Zgliczyński, a specific method for checking the conditions of

the Shilnikov criterion, whose fulfilment guarantees the existence of the Lorenz attractor, was proposed. The corresponding approach was implemented with help of computer-assisted proof methods, and thus, like the Tucker's method, it is very time-consuming.

Mixed dynamics. The discovery of mixed dynamics should be considered one of the main achievements in the theory of dynamical chaos, along with the discovery of its two classical forms, conservative chaos and dissipative chaos. From the point of view of topological dynamics, chaos in finite-dimensional deterministic systems can occur only in three different forms (conservative, dissipative, and mixed dynamics).

The oldest type of chaos is conservative. Its most well-known examples are chaotic dynamics demonstrated by non-integrable Hamiltonian systems. The discovery of conservative chaos is associated with the name of Poincaré, who, showed in 1889 that a typical property of Hamiltonian systems with two or more degrees of freedom is the existence of robust homoclinic curves for saddle periodic orbits. Such curves (orbits) are now called homoclinic Poincaré curves (orbits), and their robustness means that the stable and unstable invariant manifolds of the periodic saddle orbit intersect transversally. Poincaré noted that the existence of such orbits in Hamiltonian systems implies their fundamental non-integrability – now this phenomenon is known as the Poincaré criterion for conservative (Hamiltonian) chaos.

The discovery of dissipative chaos is usually associated with the classical paper by E. Lorenz, published in 1963. This work gave an example of a three-dimensional system demonstrating complicated non-periodic behavior of non-wandering orbits on some globally stable invariant set. This system was later called the Lorenz model, and the attracting invariant set with irregular and unstable behavior of orbits on it was called the Lorenz attractor.

Currently, conservative chaos, as well as dissipative chaos, the mathematical image of which is a strange attractor, are two of the most popular and relevant research areas in nonlinear science. These two types of chaos are objects of study not only by mathematicians, but also by specialists from various fields of natural sciences: physics, biology, chemistry, etc.

Mixed dynamics is the youngest type of dynamical chaos. It was discovered quite recently. The very phenomenon of the coexistence of an infinite set of periodic orbits of all possible types (stable, completely unstable, and saddle) and their inseparability from each other, in the sense that the closures of sets of orbits of different type have a non-empty intersection, was discovered in 1997 in the paper by Gonchenko, Turaev, and Shilnikov. In 2017, Gonchenko and Turaev, based on the Ruelle notation of an attractor, showed that the attractor and the repeller can intersect by a closed invariant set – the so-called reversible core, which is both an attractor and a repeller, and at the same time does not attract and does not repels any trajectories. In this work, in essence, the foundations of the mathematical theory of mixed dynamics were laid.

Despite the fact that mixed dynamics was discovered quite recently, a large number of models in which it is observed are already known. In numerical experiments, this phenomenon was first discovered in the papers by A. Gonchenko, S. Gonchenko, and a dissertation applicant devoted to the study of nonholonomic models of Celtic stone and Chaplygin top. After this works, it became clear that mixed dynamics is a typical phenomenon for non-integrable nonholonomic systems without a smooth invariant measure. Later, in the works of Bizyaev, Borisov, Mamaev, Kruglov, S.P. Kuznetsov, this conjecture was confirmed for a number of other nonholonomic models. It is important to note that, as we now know, models with mixed dynamics appeared long before this type of chaos was discovered. Among such models we would like

to note models of two-dimensional reversible maps considered in the works of Politi, Quispel, Roberts, and others. We especially note here the paper by Pikovsky and Topaj (2002), in which mixed dynamics was, in fact, illustrated in system governing chains of symmetrically coupled oscillators. Later, the existence of mixed dynamics in this model was established in the work of a dissertation applicant (2017).

Among the physical works on mixed dynamics, a series of recent papers by Emelyanova and Nekorkin, devoted to the study of chaotic dynamics in a system of two adaptively coupled neuron-like elements, should be noted here. The mixed dynamics found in these papers, as shown by the authors, corresponds to new types of neural-like oscillations, characterized by a specific distribution of interspike intervals. It is important to note here that in these works mixed dynamics was discovered and studied in systems of general position. Before this, all known systems with mixed dynamics belong to the class of reversible systems that are symmetric with respect to the time reversal.

Aims and tasks of the study. The aim of the dissertation work is the development of new methods for the study of multidimensional dynamical chaos and the application of these methods to the analysis of dynamical systems, which are important from both theoretical and applied points of view. To achieve these goals, the following tasks were solved:

- Development of efficiently verifiable methods for checking the pseudohyperbolicity of strange attractors of multidimensional dynamical systems.
- Construction of new examples of dynamical systems demonstrating pseudohyperbolic attractors, as well as the study of scenarios of their appearance.
- Development of scenarios for the transition from conservative and dissipative dynamics to mixed dynamics. Construction of criteria for the existence of mixed dynamics in reversible systems.
- Development of methods for the study of integrability of reversible dynamical systems.
- Study of applied problems of nonholonomic mechanics, hydrodynamics, theory of chains of interacting oscillators.
- Development of a software package that implements the created numerical methods for studying multidimensional dynamical systems.

Research methods.

For solving the above-stated set of tasks, qualitative and analytical methods of the theory of dynamical systems were applied. For the study of specific systems (nonholonomic models of rigid body dynamics, hydrodynamic models, etc.), methods of the applied theory of bifurcations, as well as numerical methods (construction of diagrams of Lyapunov exponents, continuation by a parameter, numerical methods for checking pseudohyperbolicity, the method of diagrams of symbolic dynamics, etc.) were used. Numerical methods were implemented in the C++ language within the framework of the "Computer Dynamics: Chaos" software package (patents RU 2014619001 and RU 2016660109). To speed up the work of the methods, Qt threads and CUDA API technologies were used.

Theoretical and practical significance.

Pseudohyperbolic attractors. Until recently, in theory of dynamical chaos the known examples of genuine chaotic attractors were only the uniformly hyperbolic attractors (Smale-Williams, Anosov, Plykin, etc.) and the Lorenz attractors. The theory of pseudohyperbolic attractors, which was laid down in 1998, was a very promising mathematical theory which, however, has no examples of such attractors observed in specific models. This big problem was solved in the dissertation work where four examples of wild pseudohyperbolic attractors are presented: a wild spiral attractor in a four-dimensional system of differential equations and a discrete Lorenz attractor, a figure-eight attractor, and a heteroclinic Lorenz attractor in three-dimensional maps. Thus, in addition to the hyperbolic and Lorenz attractors, a series of new pseudohyperbolic wild attractors has been added to the class of genuine attractors, which is a significant advance in the theory of dynamical chaos, in particular, and in the theory of dynamical systems, in general.

In addition to studying specific models and discovering new types of wild pseudohyperbolic attractors, the dissertation applicant proposed a set of numerical methods implemented within the framework of a software package, which makes it possible to answer one of the main questions in theory of dynamical systems: is the strange attractor observed in a numerical experiment genuinely chaotic or it is just a long transient process after which the trajectory runs away to a stable regular regime. Thus, the practical significance of the results obtained in the dissertation work is that scientists from various fields of natural science (physics, biology, chemistry, etc.) got a real opportunity to find pseudohyperbolic attractors in multidimensional systems, as well as to effectively study their dynamical properties.

Mixed dynamics. Theory of mixed dynamics, as the third form of dynamical chaos, for which a chaotic attractor intersects with a chaotic repeller, has been developed quite recently. Therefore, any discovery in this area is a significant advancement for the corresponding theory. The dissertation applicant discovered a number of new phenomena in the field of mixed dynamics theory and its applications: a new type of it – strongly dissipative mixed dynamics, as well as a number of new scenarios for the instant onset of mixed dynamics as a result of the collision of simple attractor – simple repeller and strange attractors – strange repeller. On the basis of mixed dynamics theory, a new method that makes it possible to answer questions about the integrability of multidimensional reversible systems was proposed. In particular, this method was used for solving problem of V.V. Kozlov. The discovered phenomena also made it possible to explain the emergence of the intersection of attractor – repeller in the Pikovsky-Topage model of four coupled oscillators, the instant appearance of mixed dynamics in the nonholonomic model of Suslov top, as well as in the model of two point vortices in the field of an acoustic wave.

To date, a series of models demonstrating mixed dynamics phenomenon from various applications are known. Thus, the practical significance of the corresponding results of the dissertation applicant is beyond doubt. Moreover, to solve the problems arising here, the dissertation applicant developed an original software package that implements numerical methods aimed at studying systems of various natures with mixed dynamics, and more generally, systems with all three possible types of dynamical chaos.

Provisions for the defense.

1. New methods for checking the pseudohyperbolicity of strange attractors based on direct verification of the continuity of strong-stable and central-unstable invariant subspaces.

   With the help of these methods, the pseudohyperbolicity of a number of strange attractors in three-dimensional Hénon map, as well as in the nonholonomic models of Celtic stone and Chaplygin top, was established in the dissertation work.

2. A wild spiral attractor in a four-dimensional system of ordinary differential equations, which is an extension of the classical Lorenz system.

   The first and so far the only example of a system demonstrating a wild spiral attractor is presented in this dissertation work. Its pseudohyperbolicity is established, it is shown that such attractor contains the wild hyperbolic Newhouse set. A phenomenological model of the wild spiral attractor was constructed by Turaev and Shilnikov in 1998, however, concrete examples of systems with such attractors have not been known until the work of dissertation applicant.

3. Non-orientable pseudohyperbolic heteroclinic Lorenz attractor in the three-dimensional Hénon map.

   A new example of a discrete chaotic attractor is found. Such an attractor contains a period-2 saddle orbit and homoclinic to it orbits. Pseudohyperbolicity of this attractor is established by means of the methods developed in the dissertation work; it is also shown that such an attractor can appear as a result of a local bifurcation of a fixed point with a triplet of multipliers $(-1, i, -i)$.

4. Strange attractors in the generalized Lorenz system.

   The existence of pseudohyperbolic Lorenz attractors and measure-persistent Rovella attractors (Lorenz-type quasiattractors containing a saddle equilibrium state with a negative saddle value) is numerically established in the generalized Lorenz model proposed by Lyubimov and Zaks. This system describes an averaged convection in a horizontal fluid layer under the action of high-frequency oscillations. A new criterion for the birth of the Rovella attractor under homoclinic bifurcations is proposed.

5. Chaotic dynamics and reversal phenomenon in the nonholonomic model of Chaplygin top.

   The first and so far the only example of a pseudohyperbolic figure-eight attractor is discovered, a new bifurcation scenario of its emergence from a stable point of period 2 is presented. A new type of reversal phenomenon – when a ball with a displaced center of mass, spinning in a certain way around a vertical axis, spontaneously changes the direction of rotation around this axis to the opposite – is discovered in rigid body dynamics. The discrete Shilnikov attractor is discovered in the nonholonomic model of Chaplygin top.

6. Chaotic dynamics of the nonholonomic model of Suslov top.

   It is shown that this model can demonstrate all three possible types of dynamical chaos: conservative chaos, dissipative chaos, and mixed dynamics. An original numerical method for revealing in a parameter space of a system regions corresponding to each of the three types of chaos has been developed and implemented.

7. Mixed dynamics in the Pikovsky-Topaj model of four symmetrically coupled oscillators.

   In the model under consideration the existence of mixed dynamics, i.e., the phenomenon when a strange attractor intersects with a strange repeller, is established by means on numerical identification of the absolute Newhouse domains. A new mechanism for the instant emergence of mixed dynamics as a result of the collision of a simple attractor and a simple repeller has been discovered.

8. Scenario of the instant emergence of mixed dynamics in reversible systems as a result of collision of a strange attractor with a symmetric to it strange repeller.

   A phenomenological scenario for the instant emergence of mixed dynamics is developed and its implementation on the examples of the model of two point vortices perturbed by an acoustic wave and the nonholonomic model of Suslov top is numerically established.

9. Strongly dissipative mixed dynamics.

   A new type of mixed dynamics is discovered. For this type of mixed dynamics the numerically observed attractor and repeller intersect, but at the same time sufficiently differ from each other, although according to the theory (Gonchenko, Turaev, 2017) they should almost coincide. An explanation for this phenomenon is given. It is based on the fact that singular invariant measures on the attractor and the repeller have an extremely strong asymmetry. The existence of strongly dissipative mixed dynamics is discovered in the model describing the dynamics of two point vortices perturbed by an acoustic wave.

10. Solution of the V.V. Kozlov problem of the existence of a smooth invariant measure in a nonholonomic model a disk moving on a plane.

    Using the concept of mixed dynamics, it is shown that in general case a smooth invariant measure is absent in the corresponding nonholonomic model. In the phase space of this system, very narrow regions containing periodic sources and sinks are found. The presence of such regions is a natural obstacle for the existence of a smooth invariant measure.

11. A software package for the study of chaotic dynamics in multidimensional dynamical systems.

    A software package has been developed that allows: to identify regions with conservative and dissipative chaos, as well as with mixed dynamics in the parameter space of a system; to check the pseudohyperbolicity of strange attractors; to build kneading diagrams of homoclinic bifurcations; to reveal regions with wild hyperbolic Newhouse sets in the parameter space a system; to implement new dynamical systems using the developed interface for the creating user tasks. Parallel programming technologies were used to speed up the work of the software package.

Novelty and reliability.

All results presented in the dissertation work are new. They were obtained as part of the newly created mathematical directions in dynamical chaos theory – the theory of pseudohyperbolic attractors and the theory of mixed dynamics. Accordingly, in the dissertation work, new problems were solved that could not have arisen earlier and which required the dissertation

applicant to create original qualitative and numerical methods, as well as a software package for the study of multidimensional dynamical chaos.

All results presented to the defense were published in leading peer-reviewed physical and mathematical journals, indexed in scientific databases Web of Science and Scopus with quartiles Q1 – 8 papers, Q2 – 3 papers, and Q3 – 1 paper.

Approbation of the obtained results.

The main results of the dissertation work were reported at the following international conferences and seminars:

1. Talk *"Regular and Chaotic Phenomena in the Nonholonomic Model of an Unbalanced Ball Moving on a Plane"* at the fourth international conference "Geometry, Dynamics, Integrable Systems – GDIS 2014: Bicentennial of The Great Poncelet Theorem and Billiard Dynamics", July 2014, Triest, Italy.

2. Talk *"On phenomenon of mixed dynamics in Pikovsky-Topaj model of two coupled oscillators"* at the international conference "GDHAM15 - Global Dynamics in Hamiltonian Systems", July 2015, Barcelona, Spain.

3. Talk *"Scenarios of the birth and evolution of strange attractors in the nonholonomic model of the Chaplygin top"* at the international conference "Dynamics, Bifurcations and Chaos", July 2016, Nizhny Novgorod, Russia.

4. Talk *"Variety of strange attractors in the nonholonomic model of Chaplygin top"* at the international conference on Differential Equations and Dynamical Systems, July 2016, Suzdal, Russia.

5. Talk *"Strange attractors and mixed in a problem of two vortexes"* at the international conference "Dynamics, Bifurcations and Chaos", July 2017, Nizhny Novgorod, Russia.

6. Talk *"Examples of models with mixed dynamics (how an attractor and a repeller can collide)"* at the international conference on Differential Equations and Dynamical Systems, July 2018, Suzdal, Russia.

7. Talk *"Mixed dynamics in reversible systems"* at the XVIII scientific school-conference "Nonlinear waves - 2018", February 2018, Nizhny Novgorod, Russia.

8. Invited talk *"On discrete Shilnikov attractors in a system of symmetrically coupled oscillators"* at the international conference "Shilnikov Workshop-2018", December 2018, Nizhny Novgorod, Russia.

9. Invited talk *"Wild pseudohyperbolic attractor in a four-dimensional Lorenz model"* at the international conference "Dynamics, Equations and Applications (DEA 2019)", September 2019, Krakow, Poland.

10. Invited talk *"On Pseudohyperbolic Attractors, Quasiattractors and Their Examples"*, intercollegiate seminar of Universitat Politècnica de Catalunya and Universitat de Barcelona, November 2019, Barcelona, Spain.

11. Talk *"On the merger of a chaotic attractor with a chaotic repeller leading to the mixed dynamics"* at the international conference "709. WE-Heraeus-Seminar on Quantization of Dissipative Chaos: Ideas and Means", December 2019, Bad-Honnef, Germany.

12. Invited talk *"On the merger of a strange attractor and a strange repeller leading to mixed dynamics* at the XIX scientific school-conference "Nonlinear waves - 2020", February 2020, Nizhny Novgorod, Russia.

13. Invited talk *"On methods for verification of the pseudohyperbolicity of strange attractors"* at the international conference International Conference-School Shilnikov Workshop, December 2020, Nizhny Novgorod, Russia.

14. Invited talk *"Universal Scenarios Associated with Torus Destruction Leading to Hyperchaos and Chaos with Additional Zero Lyapunov Exponents"* at the international conference SIAM Conference on Dynamical Systems Multi-Dimensional Chaos: from Theory to Applications, May 2021, Portland, Oregon, USA.

15. Invited talk *"On bifurcations of Lorenz attractors in the Lyubimov-Zaks model"*, at the international conference Mathematical Physics, Dynamical Systems and Infinite-Dimensional Analysis-2021 (MPDSIDA), July 2021, Moscow, Russia.

List of papers on the topic of the dissertation work presented for the defense.

[1*] Borisov A. V., Kazakov A. O., Sataev I. R. *The reversal and chaotic attractor in the nonholonomic model of Chaplygin's top* //Regular and Chaotic Dynamics **19(6)** (2014), pp. 718–733.

https://link.springer.com/article/10.1134/S1560354714060094

(The discovery of a new type of reversal phenomenon in the nonholonomic model of Chaplygin top, the discovery of a figure-eight attractor in this model, and the hypothesis of its pseudohyperbolicity.)

[2*] Gonchenko A. S, Gonchenko S. V., Kazakov A. O., Turaev D. *Simple Scenarios of Onset of Chaos in Three-Dimensional Maps* //International Journal of Bifurcation and Chaos **24(8)** (2014), 1440005. (25 p.)

https://www.worldscientific.com/doi/abs/10.1142/S0218127414400057

(The description of a new scenario of the emergence of a figure-eight attractor and its implementation on the example of nonholonomic model of Chaplygin top.)

[3*] Bizyaev I. A., Borisov A. V., Kazakov A. O. *Dynamics of the Suslov problem in a gravitational field: Reversal and strange attractors* //Regular and Chaotic Dynamics **20(5)** (2015), pp. 605–626.

https://link.springer.com/article/10.1134/S1560354715050056

(Numerical and qualitative studies of all three types of chaos in the nonholonomic model of Suslov top, and methods for identifying regions in the parameter space corresponding to various types of chaotic dynamics.)

[4*] Borisov A. V., Kazakov A. O., Sataev I. R. *Spiral chaos in the nonholonomic model of a Chaplygin top* //Regular and Chaotic Dynamics **21** (2016), pp. 939–954.

https://link.springer.com/article/10.1134/S1560354716070157

(Examples of various types of discrete spiral attractors in the nonholonomic model of Chaplygin top, as well as identification of the correspondence between the real types of motion of the top and the observed dynamical regimes in the mathematical model.)

[5*] Gonchenko A.S, Gonchenko S.V., Kazakov A.O., Turaev D. *On the phenomenon of mixed dynamics in Pikovsky–Topaj system of coupled rotators* //Physica D: Nonlinear Phenomena **350** (2017), pp. 48–57.

https://www.sciencedirect.com/science/article/abs/pii/S0167278916301701

(Numerical studies of the existence of mixed dynamics in the Pikovsky-Topaj model, description of scenarios of the appearance of this phenomenon, including a new scenario for the instant emergence of mixed dynamics as a result of the collision of a simple attractor and a simple repeller.)

[6*] Gonchenko A.S., Gonchenko S.V., Kazakov A.O., Kozlov A.D. *Elements of Contemporary Theory of Dynamical Chaos: A Tutorial. Part I. Pseudohyperbolic Attractors* //International Journal of Bifurcation and Chaos **28(11)** (2018), 1830036. (13 p.)

https://www.worldscientific.com/doi/10.1142/S0218127418300367

(New method for checking the pseudohyperbolicity of strange attractors and its numerical implementation; numerical evidence of the pseudohyperbolicity of the discrete Lorenz attractors in the three-dimensional Hénon map and in the nonholonomic model of Celtic stone, as well as the figure-eight attractor in the nonholonomic model of Chaplygin top.)

[7*] Kazakov A.O. *On the Appearance of Mixed Dynamics as a Result of Collision of Strange Attractors and Repellers in Reversible Systems* //Radiophysics and Quantum Electronics **61(8-9)** (2019), pp. 650–658.

https://link.springer.com/article/10.1007/s11141-019-09925-6

(Description of the phenomenological scenario of the collision of a chaotic attractor and a chaotic repeller, leading to the appearance of mixed dynamics. Implementation of this scenario in the nonholonomic model of Suslov top. Explanation of the instant transition from dissipative chaos to mixed dynamics in this model.)

[8*] Kazakov A. *Merger of a Hénon-like attractor with a Hénon-like repeller in a model of vortex dynamics* //Chaos: An Interdisciplinary Journal of Nonlinear Science **30(1)** (2020), 011105. (8 p.)

https://aip.scitation.org/doi/abs/10.1063/1.5144144

(Discovery of a new phenomenon – strongly dissipative mixed dynamics, for which the numerically observed attractor and repeller intersect, but at the same time are very different from each other. Detection of this type of mixed dynamics in the model of two point vortices perturbed by an acoustic wave. This paper was marked as an Editor's Pick.)

[9*] Gonchenko S.V., Gonchenko A.S., Kazakov A.O. *Three Types of Attractors and Mixed Dynamics of Nonholonomic Models of Rigid Body Motion* //Proceedings of the Steklov Institute of Mathematics **308** (2020), pp. 125–140.

https://link.springer.com/article/10.1134/S0081543820010101

(Numerical evidence for the appearance of mixed dynamics in a number of nonholonomic models of rigid body motion, numerical evidence of the absence of a smooth invariant measure in the nonholonomic model of a rubber disk on a plane.)

[10*] Gonchenko S. V., Kazakov A. O., Turaev D. *Wild pseudohyperbolic attractors in a four-dimensional Lorenz system* //Nonlinearity **34(4)** (2021) (31 p.)

https://iopscience.iop.org/article/10.1088/1361-6544/abc794

(Methods for checking pseudohyperbolicity, numerical evidence of pseudohyperbolicity of the wild spiral attractor, construction of various geometric models for the wild spiral attractors.)

[11*] Gonchenko S., Gonchenko A., Kazakov A., Samylina E. *On discrete Lorenz-like attractors* //Chaos: An Interdisciplinary Journal of Nonlinear Science **31(2)** (2021), 023117 (21 p.)

https://aip.scitation.org/doi/abs/10.1063/5.0037621

(Numerical evidence of the pseudohyperbolicity of a new type of attractor – the so-called heteroclinic Lorenz attractor. This paper was marked as an Editor's Pick.)

[12*] Kazakov A.O. *On bifurcations of Lorenz attractors in the Lyubimov-Zaks model* //Chaos: An Interdisciplinary Journal of Nonlinear Science **31(9)** (2021), 093118 (19 p.)

https://aip.scitation.org/doi/abs/10.1063/5.0058585

(Detection of the pseudohyperbolic Lorenz attractor and the measure-persistent Rovella attractor in the Lyubimov-Zaks model, the criterion for the birth of the Rovella attractor.)

Patents

[13*] Borisov A.V., Mamaev I.S., Kilin A.A., Kazakov A.O., Chigarev V.G. A software package *Computer dynamics: Chaos, v. 5.0 (Chaos 5.0).* – 2014. Certificate number: RU 2014619001

(Development and implementation of numerical methods for studying dynamical chaos, technical guidance for the development of the architecture and interface of the software package.)

[14*] Borisov A.V., Mamaev I.S., Kilin A.A., Kazakov A.O., Chigarev V.G., Bizyaev I.A. A software package *Computer dynamics: Chaos, v. 5.5 (Chaos 5.5).* – 2016. Certificate number: RU 2016660109

(Development and implementation of numerical methods for studying dynamic chaos, parallelization of methods using CUDA toolkit, development of a module for creating user systems, technical guidance for the development of the architecture and interface of the software package.)

2 A summary of the work: main results

The main results of the dissertation work are divided into three parts:

- pseudohyperbolic attractors;
- mixed dynamics;
- programmed complex.

2.1 Pseudohyperbolic attractors.

In the theory of dynamical chaos, strange attractors that demonstrate stable chaotic behavior when changing the parameter values of the system are of special interest. Until recently, there were very few examples of such "genuine" strange attractors: hyperbolic attractors [1] and singular hyperbolic (Lorenz-like) attractors [2, 3, 4].

A serious weakening of the hyperbolicity conditions that does not destroy the stability property of chaotic dynamics with respect to changes in the parameter values was proposed in the paper [5], where the foundations of the theory of pseudohyperbolic attractors were laid.

Let us recall the corresponding definition of pseudohyperbolicity following our paper [10*].

Definition 1 ([10*]) *Let a compact set $\mathcal{A}$ be forward-invariant with respect to an n-dimensional C^r-flow F (i.e., $F_t(\mathcal{A}) \subset \mathcal{A}$ for $t > 0$). The set $\mathcal{A}$ is called* pseudohyperbolic *if it possesses the following properties.*

a) *For each point x of $\mathcal{A}$ there exist two continuously dependent on x linear subspaces, $E_1(x)$ with $\dim E_1 = k$ and $E_2(x)$ with $\dim E_2 = n - k$, which are invariant with respect to the differential DF of the flow:*

$$DF_t E_1(x) = E_1(F_t(x)), \qquad DF_t E_2(x) = E_2(F_t(x)),$$

for all $t \geq 0$ and all $x \in \mathcal{A}$.

b) *The splitting to E_1 and E_2 is* dominated*, i.e., there exist constants $C_1 > 0$ and $\beta > 0$ such that*

$$\|DF_t(x)|_{E_2}\| \cdot \|(DF_t(x)|_{E_1})^{-1}\| \leq C_1 e^{-\beta t}$$

for all $t \geq 0$ and all $x \in \mathcal{A}$. (This means that if we have a contraction in $E_2(x)$, then any possible contraction in $E_1(x)$ is uniformly weaker than the contraction in $E_2(x)$, and if we have an expansion in $E_1(x)$, then it is uniformly stronger than any possible expansion in $E_2(x)$).

c) *The linearized flow DF restricted to E_1 stretches all k-dimensional volumes exponentially, i.e., there exist constants $C_2 > 0$ and $\sigma > 0$ such that*

$$det(DF_t(x)|_{E_1}) \geq C_2 e^{\sigma t}$$

for all $t \geq 0$ and all $x \in \mathcal{A}$.

If the pseudohyperbolic set $\mathcal{A}$ is an attractor, we call it a *pseudohyperbolic attractor*. Note that the definition 1 is a generalization of the corresponding definition from [5].

A similar definition can be given for diffeomorphisms. Just let the time variable t take discrete values, i.e., $t \in \mathbb{Z}$, and replace F_t in the above definition by the t-th iteration of a diffeomorphism f, i.e., $F_t = f^t$.

Remark 1 *In the case of diffeomorphisms, if conditions (b) and (c) of this definition are replaced with more stringent conditions:*

b') *the linearized flow DF exponentially contracts all vectors in E_2, i.e., there exist constants $B_1 > 0$ and $\sigma_1 > 0$ such that*

$$\|DF_t(x)|_{E_2}\| \leq B_1 e^{-\sigma_1 t}$$

for all $t \geq 0$ and $x \in \mathcal{A}$,

c') *DF exponentially expands all vectors in E_1, i.e., there exist constants $B_2 > 0$ and $\sigma_2 > 0$ such that*

$$\|(DF_t(x)|_{E_1})^{-1}\| \leq B_2 e^{-\sigma_2 t}$$

for all $t \geq 0$ and $x \in \mathcal{A}$,

then, we obtain the definition of hyperbolic set.

In the case of hyperbolic flows, at each point $x \in \mathcal{A}$ there is a decomposition into three subspaces. In addition to the subspaces of contraction E_2 and expansion E_1, on which the same estimations as in conditions (b') and (c') hold, there also exists the neutral subspace E_0, tangent to the trajectory.

Finding conditions which make it possible to reliably distinguish pseudohyperbolic attractors from "not genuine" strange attractors often observed in experiments – the so-called quasi-attractors [6] – is one of the main problems in theory of dynamical system and its applications.

In the series of papers presented in this thesis, we consider only attractors for which there is a uniform contraction of all vectors in the subspace $E_2(x)$. Thus, using the standard notation of the theory of normal hyperbolicity, we will call $E_2(x)$ strongly contracting subspace and denote it by $E^{ss}(x)$; the central unstable subspaces $E_1(x)$ will be denoted by $E^{cu}(x)$. Moreover, in all considered cases $\dim E^{ss} = 1$, which means that the strongly contracting subspace is one-dimensional.

2.1.1 On methods of pseudohyperbolicity verification.

In the papers [6*, 10*], the dissertation applicant proposed a new numerical method for checking the pseudohyperbolicity of strange attractors, based on a step-by-step verification of all the conditions for the definition 1. The software implementation of this method allowed the dissertation applicant to discover a number of pseudohyperbolic attractors of a new type.

In order to reliably establish pseudohyperbolicity of the numerically observed attractor the first and simplest thing to do is to calculate the spectrum of its Lyapunov exponents

$\Lambda_1 \geq \Lambda_2 \geq \cdots \geq \Lambda_n$ along a sufficiently long orbit. Then, the condition (c) of Def. 1 implies that

$$\Lambda_1 + \cdots + \Lambda_k > 0, \tag{1}$$

and the condition (b) implies that

$$\Lambda_k > \Lambda_{k+1}, \tag{2}$$

for some $k \geq 1$ and $k < n$.

Note that these conditions must be satisfied for all orbits in the attractor. An effective way of verifying this is to take just one sufficiently long, "representative" orbit in the attractor, cut it to many relatively short pieces and then check conditions (1) and (2) for each piece by means of calculation of finite-time Lyapunov exponents [7].

However, even if both of these conditions are satisfied, this still does not indicate the pseudohyperbolicity of the attractor. In this case one can easily miss small "holes" containing, for example, stable periodic orbits. These "holes" can be so small that they cannot be detected by standard numerics [8]. Therefore, in order to be sure that there are no such holes it is very important to develop the corresponding method. Such method was suggested in our paper [10*]. It consists in checking the condition (a) of the Def. 1 in addition to the conditions (b) and (c). In order to verify the condition (a) we need to make sure that the splitting into a pair of invariant subspaces *continuously* depends on a point in the attractor. This requires the construction and analysis of invariant subspaces $E^{cu}(x)$ corresponding to the Lyapunov exponents $\Lambda_1, \ldots, \Lambda_k$ and $E^{ss}(x)$, corresponding to the exponents $\Lambda_{k+1}, \ldots, \Lambda_n$.

Further, following [10*], we describe the corresponding algorithm in more detail.

In our computations we take a very long trajectory of a system, remove a sufficiently long initial segment (to get rid of the transient) and presume that the remaining part of the trajectory gives a good approximation of the attractor. Then we compute the Lyapunov exponents for this piece of the trajectory, along with the corresponding covariant Lyapunov vectors. In such approach the existence of the invariant subspaces $E^{ss}(x)$ and $E^{cu}(x)$ is automatic. So, verifying Condition (a) reduces to checking the continuous dependence $E^{ss}(x)$ and $E^{cu}(x)$ on the point x in the attractor.

This is done in the following way. We plot the graph of the distance between $E^{ss}(x)$ and $E^{ss}(y)$ as a function of the distance between x and y for every pair of points in the attractor (i.e., on the piece of the trajectory which we use for the approximation of the attractor). If $dist(E^{ss}(x), E^{ss}(y)) \to 0$ as $dist(x, y) \to 0$, then we conclude that E^{ss} depends on the point continuously. Importantly, we endow the numerically obtained E^{ss} with an orientation, invariant with respect to the linearized flow, so we measure the distance between oriented spaces $E^{ss}(x)$ and $E^{ss}(y)$.

Thus, we check more than required by the pseudohyperbolicity condition (a). Namely, we establish the existence and continuity of an *orientable* field of subspaces $E^{ss}(x)$. Such field may not exist for all pseudohyperbolic attractors (for example, for nonorientable Lorenz attractors [4, 9]). It always exists when the absorbing domain $\mathcal{D}$ (to which the pseudohyperbolicity property of the attractor is extended) is simply-connected. But for a general topology of the attractor, the orientation of E_2 may switch when continued along a non-retractable loop. This makes our method applicable to a somewhat narrower class of attractors. For the pseudohyperbolicity analysis of attractors with non-orientable field $E^{ss}(x)$, additional research is needed.

After the continuity of E^{ss} is verified, we also check the continuity of the field of subspaces E^{cu}, also endowed with an invariant orientation. If both the fields $E^{ss}(x)$ and $E^{cu}(x)$ are continuous, we conclude the pseudohyperbolicity of the attractor.

We consider only the cases when the spaces of strong contraction are one-dimensional and, thus, the subspaces $E^{cu}(x)$ have codimension 1. Therefore, the continuity of $E^{cu}(x)$ is equivalent to the continuity of the field of normals $N^{cu}(x)$ to the hyperplanes $E^{cu}(x)$. By the definition, $E^{ss}(x)$ and $N^{cu}(x)$ are line fields; introducing an orientation makes them vector fields. We build the vector fields $\vec{E}^{ss}(x)$ and $\vec{N}^{cu}(x)$ by the following numerical procedure.

We consider a system of differential equations

$$\dot{x} = F(x),\ x \in \mathbb{R}^n. \tag{3}$$

Then we take some trajectory of the system and calculate its Lyapunov exponents $\Lambda_1, \ldots, \Lambda_n$. First, we check conditions (1), (2), which in our case take the form

$$\Lambda_1 + \cdots + \Lambda_{n-1} > 0, \tag{4}$$

$$\Lambda_{n-1} > \Lambda_n. \tag{5}$$

Let $\{x_1, ..., x_m\}$ be a sequence of points on the trajectory. Next, we take an arbitrary unit vector u_m at the point x_m and define a sequence of unit vectors u_s at the points x_s, $s = 1, \ldots, m$, by the following inductive procedure: if u_s is the vector obtained on the $(m-s)$-th iteration, then u_{s-1} is defined as $u_{s-1} = U_{s-1}/\|U_{s-1}\|$, where U_{s-1} is the solution at $t = t_{s-1}$ of the variation equation

$$\dot{U} = DF(x(t))\, U \tag{6}$$

with the initial condition $U(t_s) = u_s$; here DF stands for the matrix of derivatives of F and $x(t)$ is the solution of (3) with the initial condition $x(t_s) = x_s$. We emphasize that we solve equations (3), (6) in backward time (from $t = t_s$ to $t = t_1$). In order to suppress instability in x, we use, at every step, the stored value of x_s as the initial condition, precomputed by integration of (3) in forward time. By (5) the sequence of the unit vectors u_s exponentially converges to the covariant Lyapunov vector corresponding to the Lyapunov exponent Λ_n, for almost every initial conditions u_m. Thus, if m_1, m_2, and m are sufficiently large, then the segment of the orbit $\mathcal{X}$ corresponding to $s \in [m_1, m - m_2]$ gives a good approximation to the attractor and the vectors u_s give a good approximation to $\vec{E}^{ss}(x_s)$.

We use an analogous procedure to construct vectors $\vec{N}^{cu}(x_s) = w_s$. We start with a unit vector w_0 and define, inductively, $w_{s+1} = W_{s+1}/\|W_{s+1}\|$, where W_{s+1} is the solution at $t = t_{s+1}$ of the adjoint variation equation

$$\dot{W} = -[DF(x(t))]^\top\, W \tag{7}$$

with the initial condition $W(t_s) = w_s$. Obviously, if $u(t)$ is a solution of (6) and $w(t)$ is a solution of (7), then the inner product $(u(t), w(t))$ stays constant:

$$\frac{d}{dt}(u, w) = (Au, w) - (u, A^\top w) = 0$$

(where we denote $A(t) = DF(x(t))$). Therefore, given any codimension-1 subspace orthogonal to w_0, the sequence of its iterations by variational equation (6) will remain to be orthogonal to W_s at $t = t_s$. Since for a typical choice of such subspace its iterations converge exponentially to E^{cu}, it follows that W_s gives a good approximation to $\vec{N}^{cu}(x_s)$ (orthogonal to E^{cu}) for all sufficiently large s.

The same procedure works for discrete dynamical systems. We consider a diffeomorphism $x \mapsto F(x)$ and take its trajectory $x_1, \dots, x_m$, where $x_{s+1} = F(x_s)$. Then, the vectors u_s and w_s are determined by the rule

$$u_{s-1} = \frac{DF(x_s)^{-1}u_s}{\|DF(x_s)^{-1}u_s\|}, \qquad w_{s+1} = \frac{[DF(x_s)^{\top}]^{-1}w_s}{\|DF(x_s)^{\top}]^{-1}w_s\|}.$$

Note, that the attractor of the map F can have orientable fields of subspaces $\vec{E}^{ss}$ and $\vec{N}^{cu}$, but the orientation may flip with each iteration of F. To avoid problems with that, we can simply remove from the sequence (x_s, u_s, w_s) every second term.

Finally, once the orbit x_s, $s \in [m_1, m - m_2]$, and the vectors u_s and w_s are computed, we plot the $\vec{E}^{ss}$- and $\vec{N}^{cu}$-*continuity diagrams*. These are graphs in the (ρ, φ)-plane, where for each pair of points (x_i, x_j), $m_1 \le i < j \le m - m_2$,[1] we plot a point whose coordinate ρ equals to the distance between x_i and x_j and the coordinate φ equals to the angle between u_i and u_j for the $\vec{E}^{ss}$-continuity diagram or between w_i and w_j for the $\vec{N}^{cu}$-continuity diagram.

These diagrams look like clouds of points in the (ρ, φ)-plane. If both the $\vec{E}^{ss}$ and $\vec{N}^{cu}$ clouds touch the axis φ only at the single point $(\rho, \varphi) = (0, 0)$, then we can conclude that vector fields $\vec{E}^{ss}(x)$ and $\vec{N}^{cu}(x)$ are continuous and, thus, the attractor is pseudohyperbolic.

On the other hand, if the clouds of points touch the φ-axis at nonzero φ or there is no visible gap between the cloud and the φ-axis, then, the corresponding field of subspaces is discontinuous (and hence the attractor is not pseudohyperbolic) or it is non-orientable. The latter case may happen only when the cloud touches the axis φ just at two points $\varphi = 0$ and $\varphi = \pi$. In this case, one needs more analysis in order to decide whether the attractor is pseudohyperbolic or not as it was done, for example, in [11*] (see Section 2.1.4).

2.1.2 Wild spiral attractor in four-dimensional system.

In the paper [10*], in a four-dimensional system of ordinary differential equations, the dissertation applicant discovered the first and so far the only example of a wild spiral attractor, the phenomenological model of which was proposed more than 20 years ago in the paper by Turaev and Shilnikov.

Let us recall some important definitions.

Definition 2 ([5]) *An attractor is called wild if it contains a wild hyperbolic set (together with its unstable manifold). Wild hyperbolic set [10] is a uniformly hyperbolic invariant set whose stable and unstable invariant manifolds have non-transversal intersection and this property is preserved for C^2-small perturbations.*

[1] In the case of discrete dynamical systems (maps) we consider only even indices i and j, to avoid possible problems with orientation flipping.

Definition 3 ([5]) *Wild spiral attractor – pseudohyperbolic attractor of C^r-smooth ($r \geq 4$) flow in $\mathbb{R}^n, n \geq 4$, which contains a saddle-focus equilibrium state with eigenvalues $\gamma, -\lambda \pm i\omega, -\alpha_1, \ldots, -\alpha_{n-3}$, where*

$$\gamma > 0, \quad 0 < \lambda < Re\, \alpha_j, \quad \gamma > 2\lambda.$$

Wild pseudohyperbolic attractors, unlike hyperbolic ones, admit homoclinic tangencies, but their bifurcations do not lead to the appearance of stable periodic orbits. Instead this, only bifurcations associated with the formation of non-hyperbolic periodic orbits of the saddle-saddle type, which then split into two saddles of neighboring indices are possible here.

In the paper [10*], we consider a four-dimensional system

$$\begin{cases} \dot{x} = \sigma(y - x), \\ \dot{y} = x(r - z) - y, \\ \dot{z} = xy - bz + \mu w, \\ \dot{w} = -bw - \mu z, \end{cases} \tag{8}$$

with parameters σ, r, b and μ.

Note that when $\mu = 0$ the hyperplane $w = 0$ is invariant and, in restriction onto this hyperplane, system (8) is exactly the Lorenz model. In [10*], we found a wild spiral attractor in this system when

$$\mu = 7, \sigma = 10, b = 8/3, r = 25, \tag{9}$$

see. Fig. 1a,b, and give a numerical evidence of its pseudohyperbolicity by means of the methods described in Sec. 2.1.1.

The attractor under consideration contains an equilibrium state characterized by a set of eigenvalues:

$$\lambda_1 = \tfrac{1}{2}\left(\sqrt{(\sigma-1)^2 + 4\sigma r} - \sigma - 1\right),$$
$$\lambda_{2,3} = -b \pm i\mu,$$
$$\lambda_4 = -\tfrac{1}{2}\left(\sqrt{(\sigma-1)^2 + 4\sigma r} + \sigma + 1\right).$$

At $r = 28, \sigma = 10, b = 8/3$ this gives $\lambda_1 \approx 11.83, \lambda_{2,3} = -8/3 \pm i\mu, \lambda_4 \approx -22.83$. Therefore, the space E^{ss} at the point O is one-dimensional (it corresponds to the smallest eigenvalue λ_4). By continuity of E^{ss}, would we have a pseudohyperbolic attractor the space E^{ss} would be one-dimensional at every point of the attractor. Accordingly, the space E^{cu} must be three-dimensional. This condition is not satisfied for small μ – the sum of the first three Lyapunov exponents is negative. Indeed, it is well known that the first two Lyapunov exponents for the Lorenz system at the classical parameter values are $\Lambda_1 \approx 0.906$ and $\Lambda_2 = 0$. In system (8) at $\mu = 0$ the Lyapunov exponents Λ_1 and Λ_2 remain the same and $\Lambda_3 = -8/3$. This gives $\Lambda_1 + \Lambda_2 + \Lambda_3 \approx -1.761 < 0$ and it cannot become positive for small μ.

At point (9) of the parameter space the chaotic attractor has the following set of Lyapunov exponents: $\Lambda_1 \approx 2.19, \Lambda_2 \approx 0, \Lambda_3 \approx -1.96, \Lambda_4 \approx -16.56$. Therefore, the attractor satisfies the necessary conditions (b) and (c) for pseudohyperbolicity (see Def. 1).

To establish its pseudohyperbolicity, we need to verify the last condition (a) ensuring that

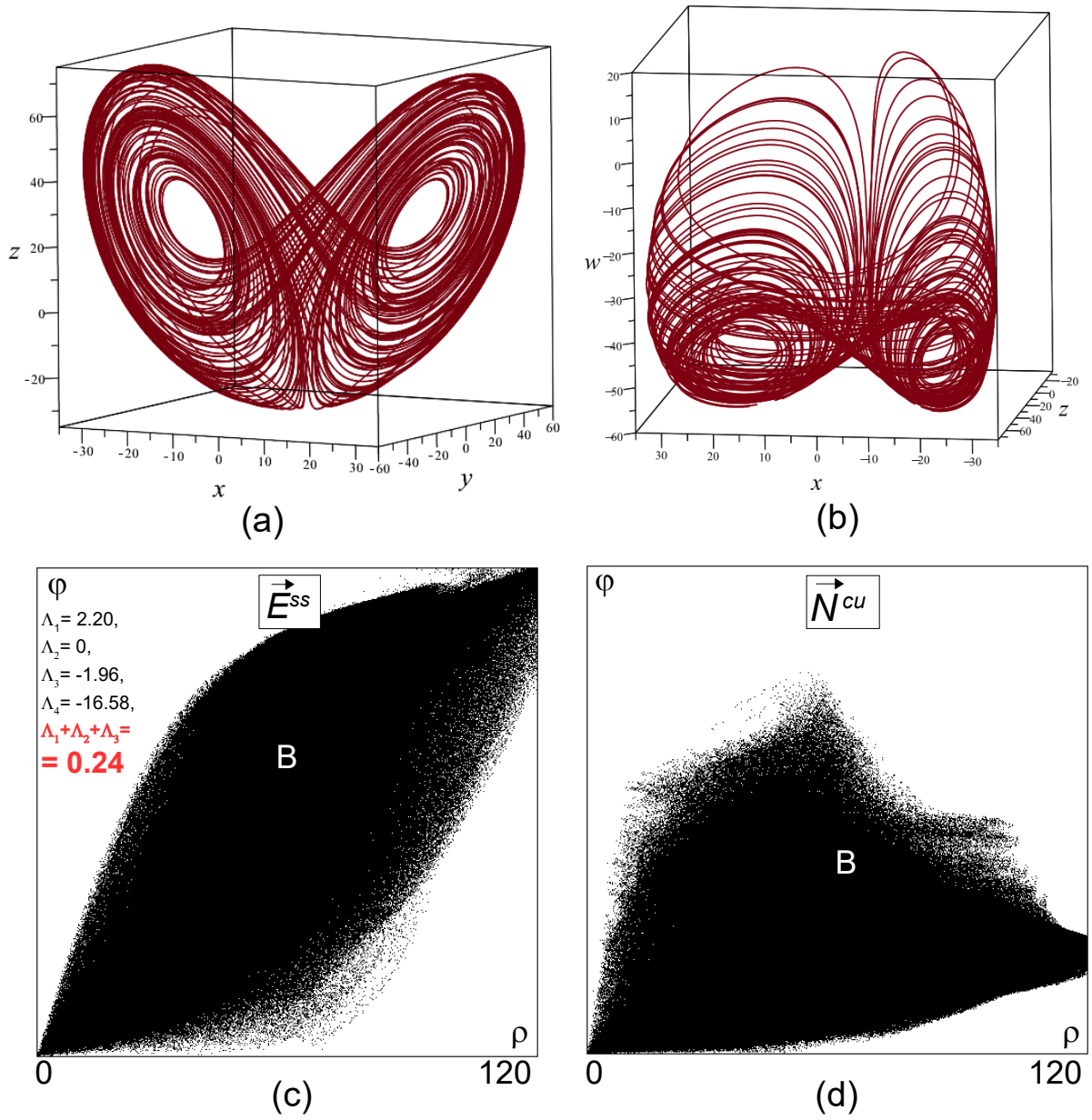

Fig. 1: (a) and (b) Projections of the strange attractor existing in system (8) at $\sigma = 10, b = 8/3, r = 25$ and $\mu = 7$ onto the (x, y, z)-plane and the (x, z, w)-plane; (c) and (d) E^{ss}- and N^{cu}-continuity diagrams confirming pseudohyperbolicity of this attractor.

the subspaces $E^{ss}(x)$ and $E^{cu}(x)$ depend continuously on the point of the attractor. We did it by computing the $\vec{E}^{ss}$- and $\vec{N}^{cu}$-continuity diagrams, as discussed in Sec. 2.1.1. The diagrams are shown in Fig. 1c,d. They are clearly show the sought continuity of E^{ss} and E^{cu}.

In addition, in [10*], it was numerically established that the attractor shown in Fig. 1 corresponds to the conditions of the Turaev-Shilnikov phenomenological model [5], and also shown that this attractor contains the wild hyperbolic Newhouse set.

2.1.3 Pseudohyperbolicity of the discrete Lorenz attractor.

In the papers [6*, 10*], pseudohyperbolicity of the discrete Lorenz attractor in a three-dimensional Hénon map was established by means of numerical methods described in the Section 2.1.1.

For the first time such an attractor was found in [11], where it was shown that in the three-dimensional Hénon map of the form

$$\bar{x} = y,\ \bar{y} = z,\ \bar{z} = M_1 + Bx + M_2 y - z^2, \tag{10}$$

where M_1, M_2, B are parameters (B is the Jacobian), the *wild discrete Lorenz attractor* exists in some region of parameter values adjoining the point $P : (M_1, M_2, B) = (1/4, 1, 1)$.

Definition 4 ([11*]) *The discrete Lorenz attractor A can be defined as*

(i) homoclinic attractor containing a saddle fixed point O with multipliers $\lambda_1, \lambda_2, \lambda_3$ such that $|\lambda_1| > 1$, $0 < |\lambda_3| < \lambda_2 < 1$, $|\lambda_1\lambda_2\lambda_3| < 1$ and the saddle index $\sigma \equiv |\lambda_1\lambda_2|$ greater than one;

(ii) Let Γ_1 and Γ_2 be the unstable separatrices of the point O, forming together with O the unstable invariant manifold $W^u(O)$, then all points belonging to the intersection $\Gamma_1 \cap W^s_{loc}(O)$ and $\Gamma_2 \cap W^s_{loc}(O)$ lie entirely on the same part of the set $W^s_{loc}(O) \backslash W^{ss}(O)$, see Fig. 2;

(iii) there is an adsorbing domain D for A that has a solid pretzel shape (a ball with two holes) and such that a closed curve $\mathcal{L}_i, i = 1, 2$, is non-contractible in D, where $\mathcal{L}_{)_i}$ is composed from a piece of Γ_i from O to the point h_i of the first intersection of Γ_i with W^s_{loc} and a simple arc between h_i and O, see Fig. 2.

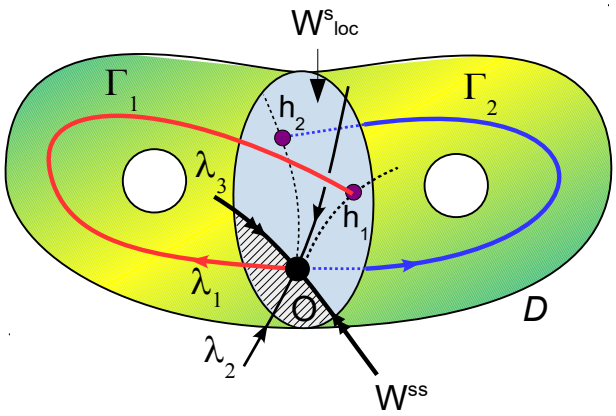

Fig. 2: Illustration for the definition 4 of the discrete Lorenz attractor.

In the paper [11], pseudohyperbolicity of the discrete Lorenz attractors was verified analytically on the basis of the fact that for parameter values close to the point P, the square of the map in some neighborhood of the saddle fixed point can be represented as the Poincaré map of the periodically perturbed Shimizu-Morioka system, which has the Lorenz attractor [12, 13]. When the perturbation is small enough (which is determined by the closeness of the parameters to the point P), then the sought pseudohyperbolicity should naturally be inherited from the Lorenz attractor, which itself is pseudohyperbolic [14]. In particular, it was shown in [15] that the property of pseudohyperbolicity of system of differential equations is also preserved under small periodic perturbations (the corresponding Poincaré maps are also pseudohyperbolic).

However, the values of the parameters $(M_1, M_2, B) = (0, 0.85, 0.7)$, at which the discrete Lorenz attractors were found in the map (10), are not at all close to the point P, near which the existence of the Lorenz attractor is theoretically justified. Therefore, the conditions for the pseudohyperbolicity of such attractors must be checked additionally. Such verification, with help of the methods described in Section 2.1.1, was done in the paper [10*]. Let us briefly describe the results of this verification.

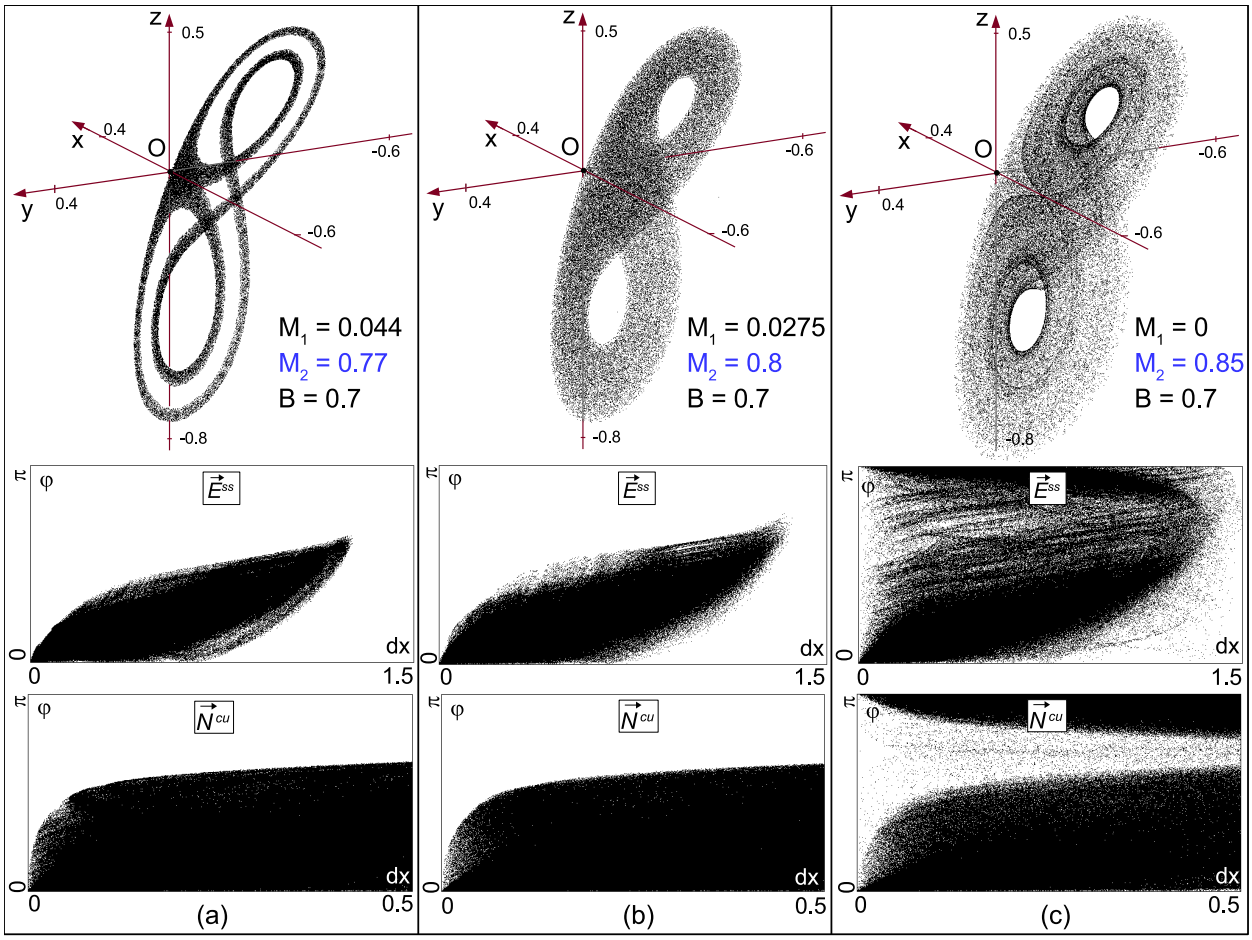

Fig. 3: Discrete Lorenz-like attractors in map (10) (top raw) and the corresponding $\vec{E}^{ss}$- (middle raw) and $\vec{N}^{cu}$- (bottom raw) continuity diagrams. Parameter values: (a) $M_1 = 0.044, M_2 = 0.77, B = 0.7$, (b) $M_1 = 0.0275, M_2 = 0.8, B = 0.7$, (c) $M_1 = 0, M_2 = 0.85, B = 0.7$. The attractor in Fig. (c) is not pseudohyperbolic.

In Fig. 3, examples of discrete Lorenz-like attractors are shown for map (10) at $B = 0.7$. The continuity diagrams were computed for every second iteration of the map (the map flips the orientation in E^{ss}, as the smallest, i.e., the strongly stable, eigenvalue of the fixed point is negative). Attractors shown in Fig. 3a and 3b exhibit the continuity of the field of subspaces $E^{ss}(x)$ and $E^{cu}(x)$, so we can conclude the pseudohyperbolicity, see also [6*] (the necessary conditions $\Lambda_1 + \Lambda_2 > 0$ and $\Lambda_2 > \Lambda_3$ were checked in [11]).

Despite the positivity of the maximal Lyapunov exponent (see [11]), the attractor presented in Fig. 3c is not pseudohyperbolic (the fields of subspaces $E^{ss}(x)$ and $E^{cu}(x)$ are not continuous). In fact, one can show that a stable periodic orbit exists at these parameter value and the "chaotic attractor" shown in this Fig. 3c is an artifact of the (very small) round-off numerical noise.

2.1.4 Discrete non-orientable heteroclinic Lorenz attractor.

In the paper [11*], a pseudohyperbolic attractor of a new type was discovered by a dissertation applicant. It was shown that in the three-dimensional Hénon map (10), in a neighborhood of the fixed point with a triplet of multipliers $(-1, +i, -i)$, pseudohyperbolic non-orientable attractors of Lorenz type can appear on the base of saddle point of period 2. The non-orientability of the attractor was proved by means of qualitative methods. The pseudohyperbolicity was established using the software package developed by the applicant that implements the method described in Section 2.1.1.

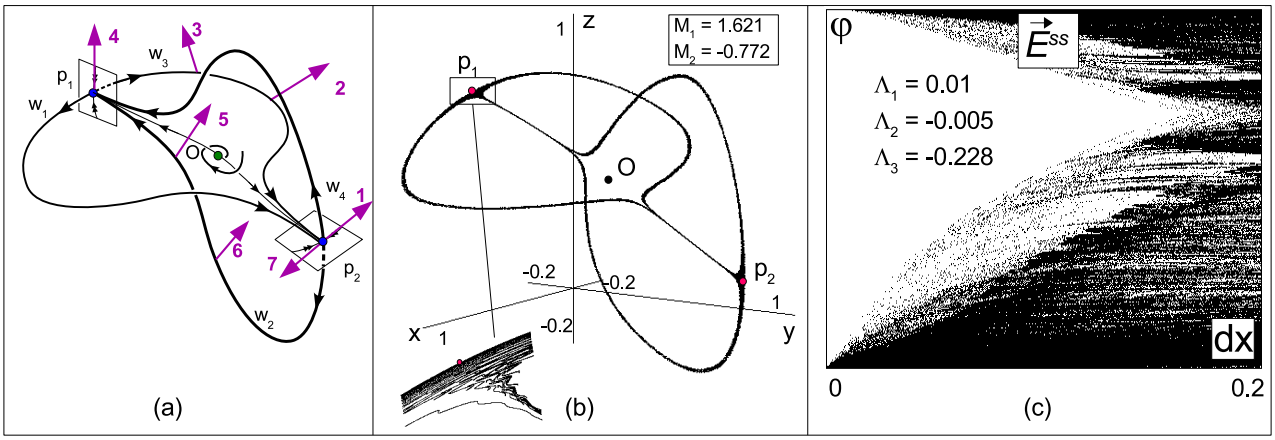

Fig. 4: Heteroclinic attractor containing the saddle point $P = (p_1, p_2)$ of period 2: (a) geometric scheme of the attractor; (b) example of such attractor in map (10) at $(M_1, M_2, B) = (1.621, -0.772, -0.8)$; here $p_1 = (a, b, a), p_2 = (b, a, b)$, where $a = 0.12, b = 0.85$; (c) E^{ss}-continuity diagram.

A skeleton scheme of such attractor is shown in Fig. 4a, it illustrates the main feature of the attractor related to the fact that all stable and unstable invariant manifolds of the points p_1 and p_2 are mutually intersect. An example of such attractor for map (10) with $B = -0.8$ is shown in Fig. 4b.

It is important to note that the period-2 heteroclinic attractors under consideration can be pseudohyperbolic. In the case of the attractor presented in Fig. 4b, its E^{ss}-continuity diagram, shown in Fig. 4c, confirms this fact. This diagram has been constructed for T^4. It contains the point $(0, \pi)$, however, this fact does not contradict to the pseudohyperbolicity of the attractor, since the points p_1 and p_2 (fixed for T^4) together with their invariant manifolds form heteroclinic cycles of non-orientable type, when passing along which the initial vector can change its direction to the opposite. In particular, this concerns vectors from the invariant spaces $E^{ss}(x)$ of Definition 1. In Fig. 4a, we illustrate this fact by showing seven successive positions of the vectors in E^{ss} near the contour $[p_2, w_3, p_1, w_2]$, while the corresponding areas in E^{cu} are lined up in the form of Möbius band.

The fact that such attractors are observed near the codimension-3 fixed point suggests that they, like the discrete homoclinic Lorenz attractors, have flow analogs. Namely, such attractors can appear in systems of differential equations near an equilibrium state with three zero eigenvalues. The discovery of the Lorenz heteroclinic attractors motivated the development of the corresponding theory; a paper on this topic is in preparation [16].

2.1.5 Discrete figure-eight and spiral attractors, and the reversal phenomenon in the nonholonomic model of Chaplygin top.

In the paper [1*], the first example of a figure-eight chaotic attractor was found in the nonholonomic model of Chaplygin top and and its pseudohyperbolicity conjecture was also proposed by the dissertation applicant; in [2*], the dissertation applicant proposed a new bifurcation scenario for the emergence of the pseudohyperbolic figure-eight attractor; in [6*], the pseudohyperbolicity of the figure-eight attractor in the nonholonomic model of Chaplygin top was established numerically by means of the software package that implements the methods described in Section 2.1.1. In the paper [4*], the discrete Shilnikov attractor was discovered in the same nonholonomic model. The discovery of a new type of reversal phenomenon in the nonholonomic dynamics of a rigid body, discovered on the example of the Chaplygin top in [1*], as well as in Suslov top in [3*] are also an important result of this dissertation work.

The phenomenological model of the *figure-eight pseudohyperbolic attractor* was proposed by Gonchenko et al. in [17]. By analogy with the discrete Lorenz attractor (see the Def. 4), the figure-eight attractor can be defined as

Definition 5 *(i) a homoclinic attractor containing a saddle fixed point O with multipliers $\lambda_1, \lambda_2, \lambda_3$, such that $\lambda_1 < -1 < \lambda_3 < 0 < \lambda_2 < 1$, $|\lambda_1\lambda_2\lambda_3| < 1$ and the saddle index $\sigma \equiv |\lambda_1\lambda_3|$ is greater than one;*

(ii) Let Γ_1 and Γ_2 be the unstable separatrices of the point O, forming (together with O) the unstable manifold $W^u(O)$, then all point belonging to the intersection $\Gamma_1 \cap W^s_{loc}(O)$ and $\Gamma_2 \cap W^s_{loc}(O)$ lie entirely in the same part of the set $W^s_{loc}(O)\backslash W^{ss}(O)$, see Fig. 5d;

(iii) there is an adsorbing domain D for A that has a solid pretzel shape (a ball with two holes) and such that a closed curve $\mathcal{L}_i, i = 1, 2$, is non-contractible in D, where $\mathcal{L}_{)_i}$ is composed from a piece of Γ_i from O to the point h_i of the first intersection of Γ_i with W^s_{loc} and a simple arc between h_i and O, see Fig. 5d.

In many details, the figure-eight attractor is similar to the discrete Lorenz attractor described above (compare Figs. 5c and 5d). Like the discrete Lorenz attractor, the figure-eight attractor is homoclinic; it contains the saddle fixed point with real multipliers satisfying the following inequality $\lambda_1 < -1 < \lambda_3 < 0 < \lambda_2 < 1$. However, the leading direction here corresponds to the negative multiplier λ_3 (in contrast to the Lorenz attractor). The necessary condition for the pseudohyperbolicity of the figure-eight attractor is $\sigma = |\lambda_1\lambda_3| > 1$, ensuring the property of expanding two-dimensional volumes at the point O.

A distinctive feature of the figure-eight attractor is that it has no flow analogues. Indeed, in the case of systems of differential equations, the geometric construction of this attractor (see Fig. 5d) ensures the existence of a two-dimensional center manifold, and thus, dynamics in the neighborhood of the saddle fixed point is effectively two-dimensional. This fact complicates the search for the figure-eight attractors.

Nevertheless, an example of such an attractor was soon discovered. The first and currently the only model demonstrating the pseudohyperbolic figure-eight attractor is the nonholonomic model describing motion of the Chaplygin top (unbalanced ball) on a plane [1*].

Equations of motion for the Chaplygin top and first integrals.

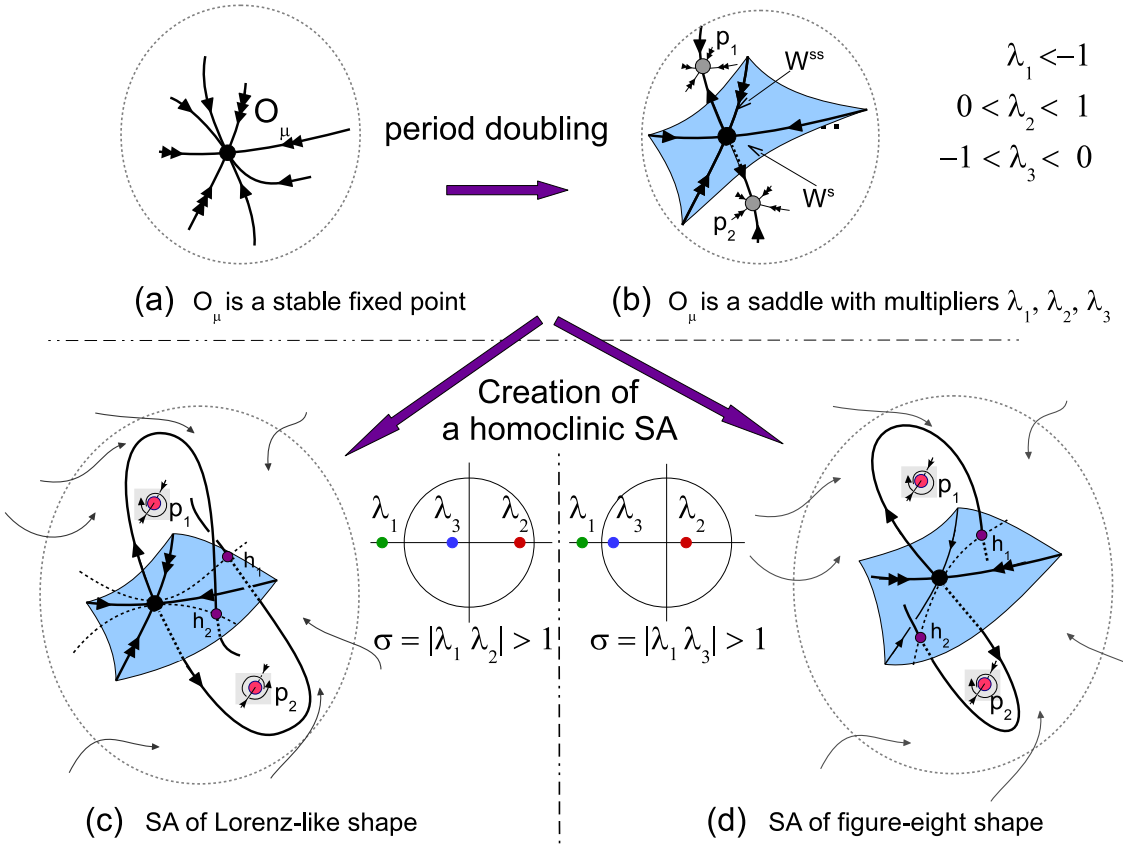

Fig. 5: Schematic representation of two scenarios of the appearance of discrete homoclinic attractors: the case of the birth of Lorenz attractor corresponds to the path $(a) \to (b) \to (c)$; the case of the birth of figure-eight attractor corresponds to the path $(a) \to (b) \to (d)$.

Equations of motion of a rigid body in the variables $\boldsymbol{M}$ and $\boldsymbol{\gamma}$, where $\boldsymbol{\gamma}$ is the vertical unit vector and $\boldsymbol{M}$ is the angular momentum relative to the point of contact, can be written as [18]:

$$\begin{cases} \dot{\boldsymbol{M}} = \boldsymbol{M} \times \boldsymbol{\omega} + m\dot{\boldsymbol{r}} \times (\boldsymbol{\omega} \times \boldsymbol{r}) + mg\boldsymbol{r} \times \boldsymbol{\gamma}, \\ \dot{\boldsymbol{\gamma}} = \boldsymbol{\gamma} \times \boldsymbol{\omega}. \end{cases} \tag{11}$$

Here m is the mass of the top and g is the acceleration of gravity. In our case, since the body is a ball with a displaced center of mass, we have

$$\boldsymbol{r} = -R\boldsymbol{\gamma} - \boldsymbol{a}, \tag{12}$$

where $\boldsymbol{a} = (a_1, a_2, a_3)$ specifies the displacement of the center of mass. In turn, the vector $\boldsymbol{M}$ is related to $\boldsymbol{\omega}$ and $\boldsymbol{r}$ by the relation

$$\boldsymbol{M} = \mathbf{I}\,\boldsymbol{\omega} + m\boldsymbol{r} \times (\boldsymbol{\omega} \times \boldsymbol{r}), \tag{13}$$

If to express the vectors $\boldsymbol{r}$, $\dot{\boldsymbol{r}}$, and $\boldsymbol{\omega}$ in terms of the vectors $\boldsymbol{M}$ and $\boldsymbol{\gamma}$, using relation (13) and (12), we can get the system of ordinary differential equations

$$(\dot{\boldsymbol{M}}, \dot{\boldsymbol{\gamma}}) = F(\boldsymbol{M}, \boldsymbol{\gamma}, \mu),$$

which depends on the vector of parameters μ characterizing the physical and dynamical properties of Chaplygin ball.

In a generic case the system (11) admits only two integrals:

$$\mathcal{E} = \frac{1}{2}(\boldsymbol{M}, \boldsymbol{\omega}) - mg(\boldsymbol{r}, \boldsymbol{\gamma}), \quad \mathcal{G} = (\boldsymbol{\gamma}, \boldsymbol{\gamma})$$

the energy and the geometric integrals. Due to normalization the geometrical integral is fixed, $\mathcal{G} = 1$. Thus, at the common level set of the corresponding integrals, the dynamics of the Chaplygin top is given by a four-dimensional system of differential equations. After choosing an appropriate cross-section, the study of the dynamics of the top is reduced to the analysis of the corresponding three-dimensional Poincaré map.

Scenario of the appearance of figure-eight attractor.

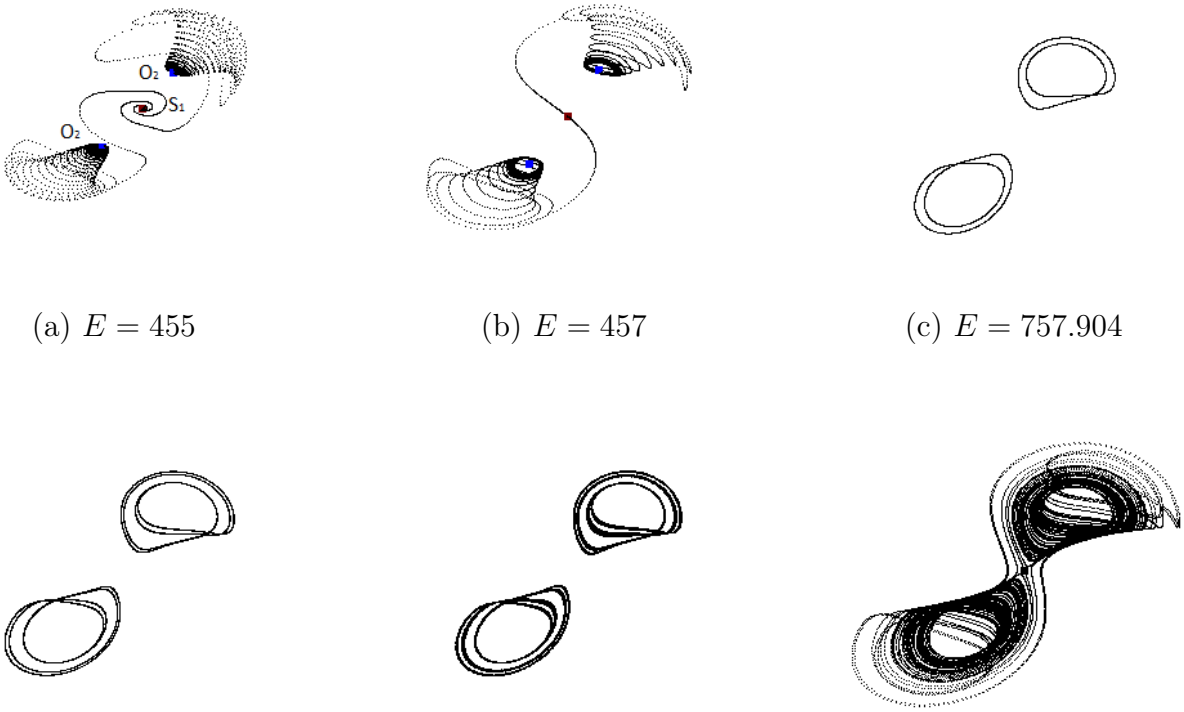

(a) $E = 455$ (b) $E = 457$ (c) $E = 757.904$

(d) $E = 457.910$ (e) $E = 457.911$ (f) $E = 457.9135$

Fig. 6: The main stages of the appearance of the figure-eight attractor in the nonholonomic model of Chaplygin top.

According to the paper [17], the first stage on the way to emergence of the figure-eight attractor can be the supercritical period-doubling bifurcation with a stable fixed point (see the transition from (a) to (b) in Fig. 5). However, in the case under consideration, the scenario of birth of the figure-eight attractor, at the initial stage, is somewhat different from [17]. The corresponding scenario was proposed in [2*]. Below, we briefly describe it.

Let us fix the parameters of the system as follows

$$I_1 = 2, I_2 = 6, I_3 = 7, m = 1, \mathrm{g} = 100, R = 3, a_1 = 1, a_2 = 1.5, a_3 = 1.9$$

and consider the energy E as a control parameter. The results of one-parameter bifurcation analysis are shown in Figure 6. At first, when $417.5 \simeq E_1 < E < E_2 \simeq 455.60$, the attractor is the point (o_1, o_2) of period 2, which is born as a result of saddle-node bifurcation together with the saddle point (s_1, s_2). It is worth noting that the Poincaré map also has the fixed saddle point S_1, which is located between o_1 and o_2, see Fig. 6a. The point S_1 is a saddle-focus up to $E \simeq E_3 = 456.162$, whereupon its unstable complex-conjugate multipliers become real negative. At $E \simeq E_4 = 456.30$ a period-2 point (s_1, s_2) merges into the saddle S_1 (as a result of the subcritical period-doubling bifurcation) and the saddle itself changes its type from (1,2) to (2,1) (its unstable manifold becomes one-dimensional). After this bifurcation the saddle S_1 has multipliers λ_1, λ_2, and λ_3, such that $\lambda_1 < -1 < \lambda_3 < 0 < \lambda_2 < 1$. Now the unstable invariant manifold of S_1 tends to a stable invariant curve L of period 2, see Fig. 6b. This curve appears via the supercritical Neimark-Sacker bifurcation from the stable cycle (o_1, o_2) at $E \simeq 455.60$.

With further increase of the parameter E the invariant curve L undergoes a series of "torus period-doubling" bifurcations (see Figs. 6c and 6d) and then gives rise to a torus-chaos attractor, see Fig. 6e). Soon after that, the unstable manifold of the saddle S_1 begins to intersect with the stable manifold, and a strange attractor which is visually similar to the figure-eight attractor is formed. Figure 6f shows a portrait of the observed attractor for $E = 457.9135$. This portrait has been obtained by iterating a point started from the neighborhood of the saddle S_1.

On pseudohyperbolicity of figure-eight attractor.

Further let us present the results of pseudohyperbolicity verification for the observed figure-eight attractor. Multipliers of the saddle fixed point S_1 for the attractor shown in Fig. 6f take the following values: $\lambda_1 = -1.00907, \lambda_2 = 0.98885, \lambda_3 = -0.99732$. Thus, the multiplier corresponding to the stable leading direction is positive, i.e., the homoclinic structure for the saddle point S_1 (see the behavior of unstable separatrices in Fig. 7d) is exactly the same as shown in Fig. 5d, and the saddle value $\sigma = |\lambda_1 \lambda_3| > 1$ provides the necessary condition for expanding the areas at the point S_1.

Lyapunov exponents of a randomly chosen trajectory in the attractor are: $\Lambda_1 \simeq 0.00063$, $\Lambda_2 \simeq 0, \Lambda_3 \simeq -0.00492$. The condition $\Lambda_1 + \Lambda_2 > 0$ also indicates its possible pseudohyperbolicity.

The continuity condition for the contracting subspace E^{ss} (conditions (a) in Def. 1) was verified in the paper [6*]. The results of the corresponding analysis are shown in Figure 7a,b. The cloud of points, in the E^{ss}-continuity diagram, touches the line $\rho = 0$ only at the point $(0, 0)$, which gives numerical evidence of the pseudohyperbolicity of the observed attractor.

Another important problem associated with the study of figure-eight attractors is related to the proof of the fact that the observed attractor is indeed homoclinic, i.e., it contains a saddle fixed point S_1, together with its unstable manifold and homoclinic orbits. In [6*], the unstable manifold of the saddle point S_1 was constructed. The pair of separatrices Γ_1 and Γ_2, forming this manifold, for two close values of the parameter E, is shown in Figures 7c,d. In contrast to the discrete Lorenz attractor, for the considered figure-eight attractors, it is not possible to find characteristic oscillations of invariant manifolds in the vicinity of the saddle fixed point, which could give a clear evidence of the occurrence of homoclinic intersections between these manifolds. However, the existence of such intersections can be established indirectly. So, at $E = 457.9125$, each of the unstable separatrices runs only around one of the components of the period-2 point (Γ_1 around o_1, while Γ_2 around o_2), see Fig. 7c. At $E = 457.9135$, a rearrangement of the unstable separatrices occurs: now each of the separatrices makes turns

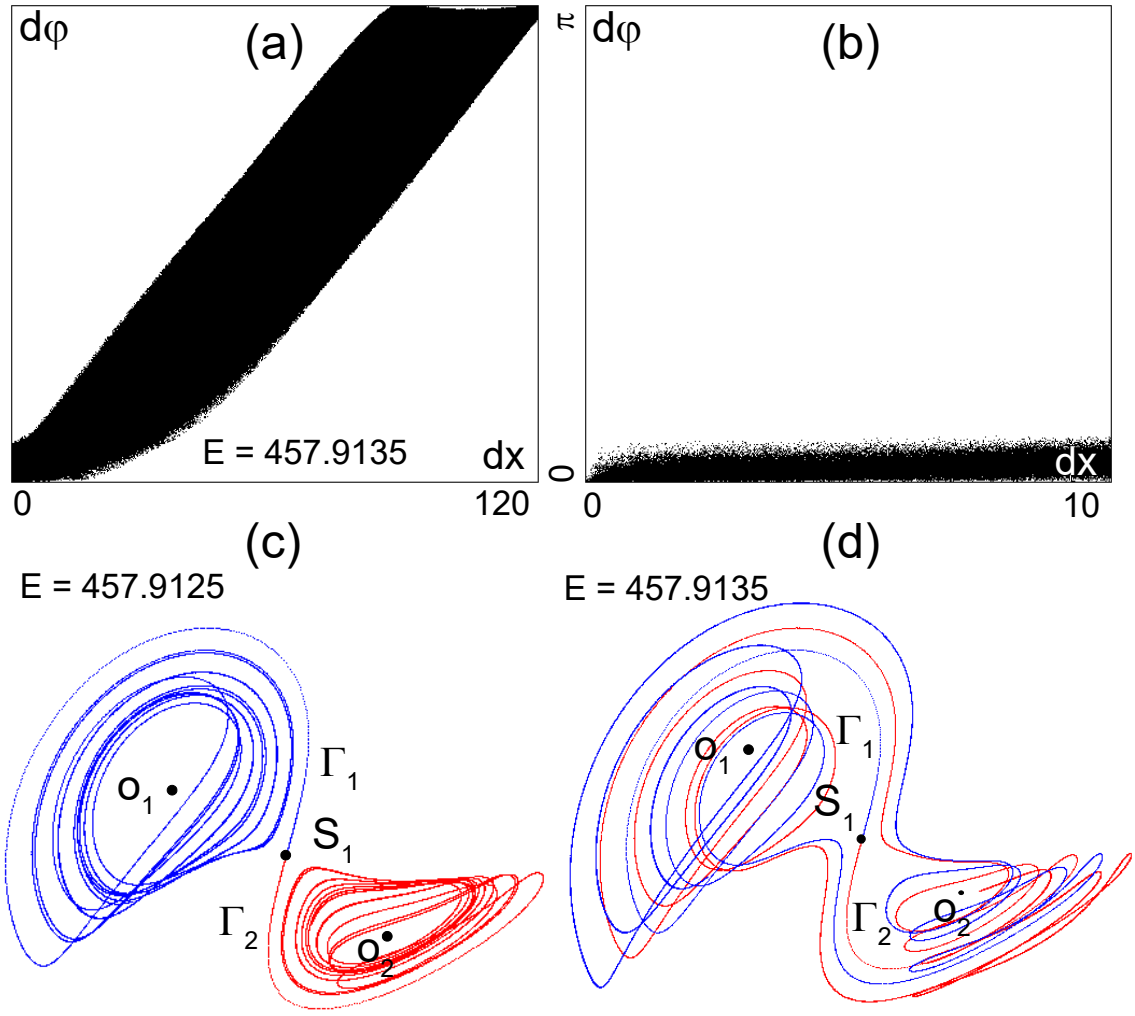

Fig. 7: (a) $E = 457.9135$, the E^{ss}-continuity diagram and (b) its enlarged fragment near the line $\rho = 0$; (c) $E = 457.9125$ and (d) $E = 457.9135$, the behavior of the unstable separatrices Γ_1 and Γ_2 of the saddle fixed point S_1: when increasing the parameter E homoclinic structure for the point S_1 appears.

both around the point o_1 and around the point o_2, passing through a certain small neighborhood of the saddle point S_1, see Fig. 7d. Such behavior confirms the existence of intersections between the unstable and stable manifolds of the saddle point S_1 at some subsegments on the interval $E \in (457.9125, 457.9135)$, i.e., the attractor under consideration is indeed homoclinic.

Discrete Shilnikov spiral attractor.

In the paper [4*], in the nonholonomic model of the Chaplygin top, a discrete Shilnikov spiral attractor was discovered – the third type of discrete homoclinic attractors, the theory of which was laid in [17].

Definition 6 *Discrete Shilnikov spiral attractor is a homoclinic attractor which contains a saddle-focal fixed point with the two-dimensional unstable invariant manifold.*

This attractor was found in system (11) at the following parameter values:

$$I_1 = 2, I_2 = 6, I_3 = 7, m = 1, \mathrm{g} = 100, R = 3, a_1 = 1, a_2 = 1.5, a_3 = 0.655, E = 422.70068.$$

Figure 8a shows a phase portrait of the corresponding attractor on the three-dimensional Poincaré map of a secant $M_1 = 0$. Figure 8b shows the behavior of the one-dimensional stable

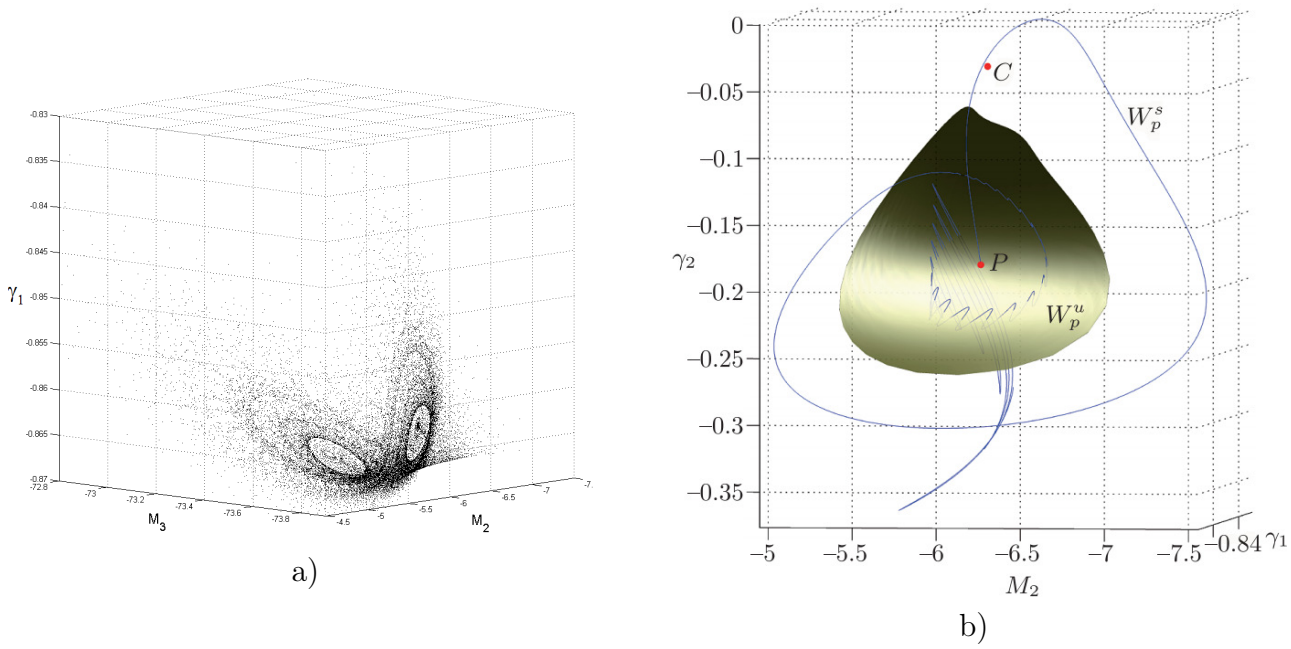

Fig. 8: (a) Phase portrait for the discrete Shilnikov spiral attractor on the Poincaré map, (b) its homoclinic structure.

manifold $W^s(P)$ as well as the unstable manifold $W^u(P)$ in some neighborhood of the saddle-focus point P. Homoclinic intersections between these manifolds confirms the "homoclinic nature" of the observed attractor.

The set of Lyapunov exponents for the attractor is $\Lambda_1 = 0.0218, \Lambda_2 = 0.0000, \Lambda_3 = -0.113$. The correlation dimension of the attractor in the Poincaré map is $D_{cor} = 2.12 \pm 0.03$. It coincides well with the Lyapunov dimension estimated according to Kaplan and Yorke: $D_{K-Y} = 2 + \Lambda_1/|\Lambda_3| \approx 2.19$.

The reversal phenomenon.

Another nontrivial phenomenon observed in system (11) is the reversal effect: when a top, twisted in a certain way around a vertical axis, spontaneously reverses the direction of rotation around this axis. Previously, similar phenomenon was observed for a Celtic stone – a solid body having rounded surface and possessing a dynamical asymmetry in mass distribution. The reversal phenomenon for the Celtic stone was explained by means of the study of its nonholonomic model. In the paper [1*], the similar effect was found in the nonholonomic model of the Chaplygin top.

Note that equations (11) are reversible with respect to the involution

$$R_0 : \boldsymbol{M} \to -\boldsymbol{M}, \boldsymbol{\gamma} \to \boldsymbol{\gamma}, t \to -t, \tag{14}$$

responsible for the reversal of angular momentum of the body relative to the contact point (and hence the angular velocities of the ball $\boldsymbol{\omega}$). Due to this property, for each asymptotically stable dynamical regime in the system, there is a symmetric analogue – an unstable regime, with angular velocities opposite in sign.

The analysis of equilibrium states in system (11) shows that, for certain parameter values, this system has an asymptotically stable equilibrium and a completely unstable equilibrium. Stable equilibrium corresponds to the rotation of the ball around a certain vertical axis with

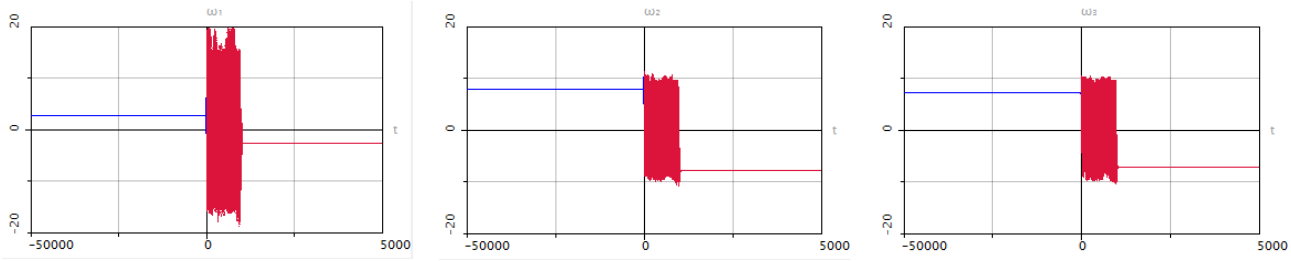

(a) $\omega_1(t)$ (b) $\omega_2(t)$ (c) $\omega_3(t)$

Fig. 9: Time series for the components of angular velocity at the following parameter values: $I_1 = 2, I_2 = 6, I_3 = 7, m = 1, \mathrm{g} = 100, R = 3, a_1 = 1, a_2 = 1.5, E_0 = 500, a_3 = 1$.

angular velocities $(\omega_1^*, \omega_2^*, \omega_3^*)$, and unstable equilibrium corresponds to the rotation of the ball around the same axis with angular velocities $(-\omega_1^*, -\omega_2^*, -\omega_3^*)$. Thus, when starting with the initial conditions near the unstable equilibrium state, the Chaplygin top, after some (maybe long) transient process, approaches a neighborhood of the stable equilibrium and continues to rotate stably around the same axis in the opposite direction. Figure 9 shows the evolution of the angular velocities of the top at the corresponding transition.

2.1.6 Lorenz and Rovella attractors in the Lyubimov-Zaks system.

In the paper [12*], the existence of the pseudohyperbolic Lorenz attractor, as well as the Rovella attractor, in the Lyubimov-Zaks model was numerically established by the dissertation applicant. Also in this work, a new criterion of the appearance of the Rovella attractor was proposed.

Recall that the Lorenz attractor, first discovered in the system of three differential equations by E. Lorenz in [2], is the first example of a "genuine" chaotic attractor that is not hyperbolic. The theory of such attractors was developed in the 70s-80s years in the works of Guckenheimer-Williams [19, 20], Afraimovich-Bykov-Shilnikov [3, 4], etc. Here we will use the following definition of the Lorenz attractor.

Definition 7 ([3, 4]) *The Lorenz attractor is an attractor of a three-dimensional system of differential equations, the Poincaré map of which satisfies the conditions of geometric model of Afraimovich-Bykov-Shilnikov.*

It is important to note that among other definitions of the Lorenz attractor, Definition 7 is the most convenient, since the conditions proposed by Afraimovich, Bykov, and Shilnikov are effectively verifiable. By means of verification of exactly these condition W. Tucker proved the existence of the Lorenz attractor in the classical Lorenz system. Analytical verification of these conditions for specific systems of differential equations, as a rule, is not possible. In his work [14], Tucker checked them using computer-assisted proof methods.

Besides directly checking the conditions of the Afraimovich-Bykov-Shilnikov model, the existence of the Lorenz attractor can be established by means of verification of the so-called *Shilnikov criteria* [21]. These criteria make it possible to establish the existence of the Lorenz attractor in an open region of parameter values analysing some characteristics of only one trajectory of the system – the homoclinic loop of the saddle equilibrium state. In such a way,

the existence of the Lorenz attractor was established by A. Shilnikov in the well-known Shimizu-Morioka system [12, 13].[2]

In the paper [12*], by means of checking the conditions of the Shilnikov criterion, the existence of the Lorenz attractor was shown in system

$$\begin{cases} \dot{x} = \sigma(y - x) + \sigma D y(z - r) \\ \dot{y} = x(r - z) - y \\ \dot{z} = xy - bz, \end{cases} \tag{15}$$

proposed in [23] as a generalization of the well-known classical Lorenz model [2]. This system describes convection in a horizontal liquid layer under the action of high-frequency vibrations. Here b, r, σ are the Lorenz model parameters, and D is a vibration parameter.

A detailed description of this criterion can be found in book [24]. For convenience we recall it in the three-dimensional case. Let us consider a three-dimensional system of differential equation possessing a saddle equilibrium O with eigenvalues $\gamma, \lambda_1, \lambda_2$, such that:

$$\gamma > 0 > \lambda_1 > \lambda_2.$$

Assume that this system is invariant with respect to a symmetry $\mathbb{S}$, such that O is a symmetric equilibrium ($\mathbb{S}\, O = O$) and the eigenvectors V_γ and V_{λ_1} corresponding to the eigenvalues γ and λ_1 are $\mathbb{S}$-invariant: $\mathbb{S}\, V_\gamma = -V_\gamma$ and $\mathbb{S}\, V_{\lambda_1} = V_{\lambda_1}$. We also assume that this symmetry implies a symmetry of two unstable separatrices Γ_1 and Γ_2 touching the eigenvector V_γ at point O, i.e., $\mathbb{S}\, \Gamma_1 = \Gamma_2$ and $\mathbb{S}\, \Gamma_2 = \Gamma_1$. Further assume that the following three conditions for the system are fulfilled:

1. both unstable separatrices Γ_1 and Γ_2 return to O at $t \to +\infty$ touching the eigenvector V_{λ_1}, i.e., a homoclinic butterfly bifurcation to O is created;

2. the saddle index ν of O is equal to one, i.e., $\nu = -\lambda_1/\gamma = 1$;

3. the separatrix value A satisfies the condition

$$0 < |A| < 2. \tag{16}$$

According to L.P. Shilnikov [21], bifurcations of such system lead to the birth of the Lorenz attractor.

It is worth noting that in the class of $\mathbb{S}$-symmetric systems under consideration, conditions 1 and 2 correspond to a codimension-2 bifurcation. Thus, if to embed such a system into a two-parameter family $F_{\mu,\nu}$ of systems for which varying μ and ν we can independently split the homoclinic butterfly and change the saddle index near 1 we can formulate the Shilnikov criterion more precisely. If condition (16) is fulfilled in the codimension-2 point (when system $F_{\mu,\nu}$ has a homoclinic butterfly with a neutral saddle), then in the (μ, ν)-parameter plane there exists an open region with the Lorenz attractor of the Afraimovich-Bykov-Shilnikov model and the point $(\mu, \nu) = (0, 1)$ belongs to its boundary.

[2] A rigorous proof of this fact is given in [22].

In a small neighborhood of the point S the normal form for studying the Lorenz attractor is determined by the following one-dimensional map [24]:

$$X_{n+1} = (-\mu + A|X_n|^\nu + o(|X_n|^\nu))\text{sign}(X_n). \tag{17}$$

Here μ is a separatrix splitting parameter for the symmetric butterfly, ν is the saddle index of the equilibrium, and A is the separatrix value. In order to check the fulfilment of the Shilnikov criterion, it is necessary to show that all three of the above conditions are satisfied. The first two conditions are easily verified by standard methods of bifurcation analysis (for example, using the MatCont software package). In order to estimate the separatrix value at point S, the following procedure was applied.

A test point is taken in a chaotic region very close to the point S in the parameter plane. For this point, the one-dimensional map $X_{n+1} = f(X_n)$ is calculated from the numerically constructed two-dimensional Poincaré map. Next, based on the one-dimensional map, the value of parameter μ is determined. The parameter ν is easily defined as the saddle index of the equilibrium state O of system (15). The last parameter, A, is chosen using the least squares method in order to provide the best fit between the numerically obtained graph $f(X)$ and the one-dimensional map (17).

The described procedure allows one to obtain a sufficiently accurate estimation for the separatrix value at point S. In the paper [12*], it was shown that in system (15) the separatrix value A is approximately equal to 1.19. Therefore, according to the Shilnikov criterion, the region with the Lorenz attractor adjoins to the point S.

Criterion for the birth of the Rovella attractor.

The results of numerical study show that in system (15), Lorenz-like attractors also exist in the parameter region where the saddle equilibrium has a negative saddle value. The theory of such attractors was developed by A. Rovella in [25] where it was shown that under certain conditions such attractors exist on nowhere dense sets with positive Lebesgue measure.

Until recently, examples of specific systems of differential equations demonstrating the Rovella attractors were unknown. Moreover, in the paper [26] the problem of finding an example of a system with such an attractor was noted as one of the urgent problems of nonlinear dynamics. In the paper [12*] by dissertation applicant, the existence of the Rovella attractor was shown for system (15). Moreover, a criterion for the appearance of such attractors was proposed.

Our preliminary analysis shows that if to replace condition (16) with the condition

$$|A| > 1 \tag{18}$$

while keeping the remaining conditions from the Shilnikov criterion unchanged, then bifurcations of such a system lead to the birth of the Rovella attractor. More precisely, following statement is true.

Conjecture 1 (RA-conjecture) *If condition (18) is fulfilled at the codimension-2 point (when system $F_{\mu,\nu}$ has a homoclinic butterfly with a neutral saddle), then in the (μ, ν)-parameter plane there exists a nowhere dense closed set of positive Lebesgue measure which corresponds to the existence of the Rovella attractor, and the point $(\mu, \nu) = (0, 1)$ belongs to its boundary.*

Remark 2 *For the case $|A| > 2$, with additional restrictions on the eigenvalues of the saddle equilibrium, this statement was proved in [26].*

2.2 Mixed dynamics.

The second part of the series of papers presented in the dissertation work is devoted to the development of mixed dynamics theory and qualitative and numerical methods of its research and applications.

At the present time, three independent and different forms of dynamical chaos of smooth finite-dimensional systems can be distinguished: "dissipative chaos", "conservative chaos" and "mixed dynamics". Dissipative chaos is characterized by the existence of a strange attractor in the system – a nontrivial attractive closed invariant set lying in the phase space of the system inside some absorbing region, into which all orbits crossing the boundary of this region enter. Unlike dissipative chaos, conservative chaos is spread over the entire phase space – in this case, all points are non-wandering. In terms of attractors, $\mathcal{A}$, and repellers (attractors in time reversal), $\mathcal{R}$, which, according to the well-known Conley theorem, exist for any system with a compact phase space, condition $\mathcal{A} \cap \mathcal{R} = \emptyset$ holds for dissipative chaos, while $\mathcal{A} = \mathcal{R}$ in the case of conservative chaos.

Mixed dynamics is a new type of chaos characterized by the fact that stable elements of dynamics (for example, stable periodic orbits) coexist with completely unstable ones, moreover, they are inseparable from each other. Formally, mixed dynamics satisfies conditions $\mathcal{A} \cap \mathcal{R} \neq \emptyset$ and $\mathcal{A} \neq \mathcal{R}$ [27, 28], which are complementary to the above conditions for conservative and dissipative chaos.

Soon after the appearance of the concept of mixed dynamics, the first examples of dynamical systems (including systems from applications) exhibiting this type of dynamical chaos were found in the works of the dissertation applicant. So, mixed dynamics was discovered in problems of nonholonomic mechanics in [29, 30, 3*, 7*, 9*], in chains of interacting oscillators suggested by Pikovsky and Topaj [5*], in the problems of vortex dynamics [8*], etc. In the first two cases, mixed dynamics was close to the conservative chaos, and in order to give numerical evidence of its existence, it was necessary, first of all, to determine the dissipative elements of the dynamics, which in itself was a difficult task. In particular, this concerned the model governing motion of an unbalanced disk on a plane (in which dissipation manifested itself on extremely small scales), see section 2.2.5. In the case of the model of interacting vortices, the situation was completely different: a strongly dissipative mixed dynamics was discovered in [8*]. In this case, the numerically obtained chaotic attractor and chaotic repeller are very different from each other, although according to the theory [27, 28] they should almost coincide. An explanation of this phenomenon is given in [8*], see section 2.2.4.

2.2.1 Three types of chaos in the nonholonomic model of Suslov top.

The model of Suslov top – a heavy unbalanced body with a fixed point, subject to a nonholonomic constraint that prohibits the rotation of the body around some selected axis – is one of the simplest non-integrable models of nonholonomic mechanics. In the paper [3*] by dissertation applicant it was shown that, depending on the choice of parameter values, this model can demonstrate all three types of dynamical chaos: conservative (Hamiltonian) chaos,

dissipative chaos (separated from each other by a strange attractor and a strange repeller) and mixed dynamics.

Equations of motion and first integrals.

Let us choose a coordinate system $Oxyz$, attached with the body in the following manner: the origin O coincides with the fixed point of the body, the Oz-axis is collinear with the chosen fixed vector $\boldsymbol{e}$, and the axes Ox and Oz are directed in such a way that the components I_{12} and I_{21} of inertia tensor vanish. Then, the nonholonomic constraint $(\boldsymbol{\omega}, \boldsymbol{e}) = 0$, prohibiting rotation around a given axis $\boldsymbol{e}$, takes the simple form: $\omega_3 = 0$. In this case, the system of equations governing the angular velocity $\boldsymbol{\omega} = (\omega_1, \omega_2, 0)$ and the orientation $\boldsymbol{\gamma} = (\gamma_1, \gamma_2, \gamma_3)$, where γ_1, γ_2, and γ_3 are the projections of the vertical vector $\boldsymbol{\gamma}$ onto the axes Ox, Oy, and Oz, respectively, is determined as follows [3*]:

$$\begin{aligned} I_{11}\dot{\omega}_1 &= -\omega_2(I_{13}\omega_1 + I_{23}\omega_2) - mgc_3\gamma_2 + mgc_2\gamma_3, \\ I_{22}\dot{\omega}_2 &= \omega_1(I_{13}\omega_1 + I_{23}\omega_2) - mgc_1\gamma_3 + mgc_3\gamma_1, \\ \dot{\gamma}_1 &= -\gamma_3\omega_2, \\ \dot{\gamma}_2 &= \gamma_3\omega_1, \\ \dot{\gamma}_3 &= \gamma_1\omega_2 - \gamma_2\omega_1. \end{aligned} \tag{19}$$

Here, I_{11}, I_{22}, I_{13}, and I_{23} are the nonzero elements of the inertia tensor of the body, m is the top mass, g is the gravitational acceleration, and the vector $\boldsymbol{c} = (c_1, c_2, c_3)$ specifies the displacement of the center of mass of the top with respect to the sphere center O.

The above-written system of equations possesses the energy and geometric integrals

$$\begin{aligned} E &= \tfrac{1}{2}(I_{11}\omega_1^2 + I_{22}\omega_2^2) - mg(\boldsymbol{c}, \boldsymbol{\gamma}), \\ G &= (\boldsymbol{\gamma}, \boldsymbol{\gamma}). \end{aligned} \tag{20}$$

The value of geometric integral is always fixed, such that $G = 1$ and the value of energy integral $E = h$ is considered as another parameter in the system. System (19) on the common level of integrals (20) specify the three-dimensional flow on a certain compact three-dimensional manifold. To parametrize this flow, by analogy with [3*], we use the variables γ_2, ω_1, and γ_1, expressing ω_2 and γ_3 in terms of integrals (20). Then, choosing $\gamma_1 = const$ as a secant, we obtain the two-dimensional Poincaré map

$$(\bar{\gamma}_2, \bar{\omega}_1) = P(\gamma_2, \omega_1).$$

Further, let us fix the parameters

$$h = 101, m = 1, \mathrm{g} = 10, I_{11} = 3, I_{22} = 4, I_{13} = 0, c_1 = 0, c_2 = 0, c_3 = 10$$

and consider I_{23} as the control parameter.

Numerical results.

According to the paper [31], when $I_{23} = I_{13} = 0$, system (19) admits a smooth invariant measure ensuring the fulfilment of condition $\mathcal{A} = \mathcal{R}$. The Poincaré map in this case is shown in the Figure 10a. The observed chaotic dynamics here is conservative.

When $I_{23} > 0$, an asymmetry between the attractor and repeller arises, see Fig. 10b. In

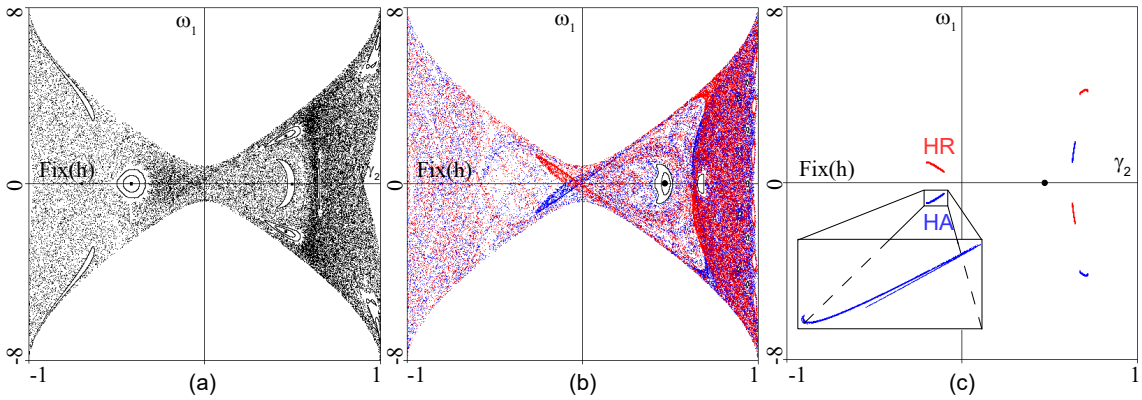

Fig. 10: Three types of chaos in the nonholonomic model of Suslov top; (a) $I_{23} = 0$ – conservative chaos, (b) $I_{23} = 0.9$ – mixed dynamics, and (c) $I_{23} = 0.908$ – the strange attractor and strange repeller are separated from each other.

[3*] it was shown that in this case, symmetry-breaking bifurcations occur inside the region with chaotic dynamics. Due to these bifurcations, periodic elliptic points become saddle points, and in their neighborhood the pairs of stable and completely unstable points of the same period are born. In the case under consideration, the conditions $\mathcal{A} \cap \mathcal{R} \neq \emptyset$ and $\mathcal{A} \neq \mathcal{R}$ are satisfied and, thus, mixed dynamics is observed.

Figure 10c shows the third possible case when $\mathcal{A} \cap \mathcal{R} = \emptyset$. Here the strange attractor HA is clearly separated from the strange repeller RH. In this case, a strange attractor (repeller) appears via the cascade of period-doubling bifurcations with a stable (unstable) point of period 3.

Also in the paper [3*] it was noticed that the mixed dynamics is characterized by the property of compression of the averaged phase volumes along the typical orbits in the attractor. Moreover, this compression is much weaker than the compression of averaged volumes in the case of a strange attractor and a strange repeller separated from each other. This property is easily verified using the standard scheme of calculation of Lyapunov exponents [32]. Based on this, a method for identification in the parameter space of a system of regions corresponding to conservative chaos, dissipative chaos and mixed dynamics is proposed. Let $\Lambda_1 \geq \Lambda_2 \geq ... \geq \Lambda_n$ be the spectrum of Lyapunov exponents of n-dimensional system. Depending on the value of sum of the Lyapunov exponents $\Sigma = \Lambda_1 + \Lambda_2 + ... + \Lambda_n$, which describes the averaged divergence along the orbits, the following classification of chaotic regimes is constructed:

- $\Lambda_1 > 0, \quad |\Sigma| \leq \varepsilon_1 \approx 0$ – conservative chaos;
- $\Lambda_1 > 0, \quad \varepsilon_1 < |\Sigma| \leq \varepsilon_2$ – mixed dynamics;
- $\Lambda_1 > 0, \quad \varepsilon_2 < |\Sigma|$ – strange attractor.

Here ε_1 and ε_2 are experimentally determined threshold values. For the Suslov top, $\varepsilon_1 = 0.0001$ and $\varepsilon_1 = 0.01$. The corresponding diagram of Lyapunov exponents for system (19) on the parameter plane (I_{23}, E) is shown in Figure 11.

It is important to note that the presented above variety of dynamical regimes in system (19) can be observed when varying only one parameter (for example, the energy parameter E). This feature makes it possible to use this model for studying bifurcation scenarios accompanying the transition between these regimes in one-parameter families. Scenarios of the transition from

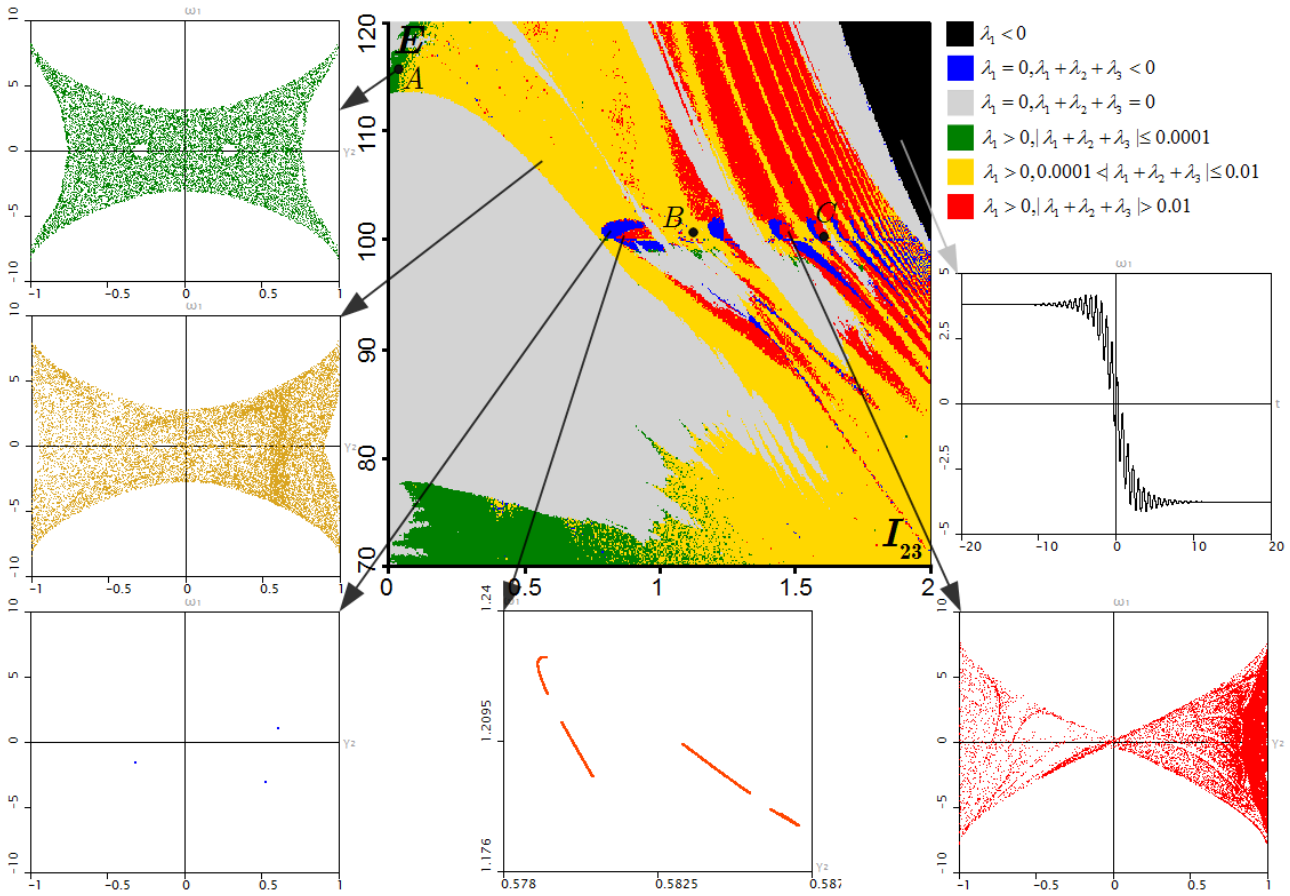

Fig. 11: Lyapunov diagram and characteristic phase portraits in system (19) for various values of the parameters I_{23} and E.

conservative chaos to mixed dynamics, as well as from dissipative chaos to mixed dynamics, are studied in [7*], see also Section 2.2.3.

2.2.2 Mixed dynamics in the Pikovsky-Topaj model.

In the paper [5*], for the Pikovsky-Topaj model, the existence of mixed dynamics, by means of numerical identification of the absolute Newhouse domains, has been established. A new mechanism for the instant appearance of mixed dynamics as a result of the collision of a simple attractor with a simple repeller has been discovered.

The Pikovsky-Topaj system describing the dynamics of a chain of coupled oscillators is the first example of a dynamical system in which the authors paid attention to the possibility of overlapping of a chaotic attractor and a chaotic repeller in numerical experiments [33]. However, the current state of affairs in theory of dynamical systems at that time did not allow to explain this phenomenon. The numerical evidence of the fact that the observed phenomenon is explained by the appearance of mixed dynamics in the system was given by us recently in the paper [5*].

The authors of [33] considered the following system:

$$\begin{aligned} \dot{\psi}_1 &= 1 - 2\varepsilon \sin \psi_1 + \varepsilon \sin \psi_2 \\ \dot{\psi}_2 &= 1 - 2\varepsilon \sin \psi_2 + \varepsilon \sin \psi_1 + \varepsilon \sin \psi_3 \\ \dot{\psi}_3 &= 1 - 2\varepsilon \sin \psi_3 + \varepsilon \sin \psi_2. \end{aligned} \tag{21}$$

Here $\psi_i \in [0, 2\pi)$, $i = 1, 2, 3$, are angular variables, and the parameter ε corresponds to the magnitude of coupling between elements. Such a choice of coupling in (21) makes the system reversible with respect to the reversal of time $t \to -t$ and involution R:

$$\psi_1 \to \pi - \psi_3 \ , \ \ \psi_2 \to \pi - \psi_2 \ , \ \ \psi_3 \to \pi - \psi_1. \tag{22}$$

For analytical and numerical studies of system (21) it is convenient to introduce the following change of coordinates

$$\xi = \frac{\psi_1 - \psi_3}{2}, \ \ \eta = \frac{\psi_1 + \psi_3 - \pi}{2}, \ \ \rho = \frac{\psi_1 + \psi_3 - \pi}{2} + \psi_2 - \pi,$$

and time $dt_{new} = (2 + \varepsilon \cos(\rho - \eta))dt$ and rewrite system (21) in the form of a non-autonomous time-periodic (with period 2π) system of two differential equations

$$\begin{aligned} \dot{\xi} &= \frac{2\varepsilon \sin\xi \sin\eta}{2 + \varepsilon\cos(t - \eta)}, \\ \dot{\eta} &= \frac{1 - \varepsilon\cos(t - \eta) - 2\varepsilon\cos\xi\cos\eta}{2 + \varepsilon\cos(t - \eta)}. \end{aligned} \tag{23}$$

Note that system (23) is reversible with respect to the change of coordinates

$$R: \quad \xi \to \xi, \ \ \eta \to -\eta \tag{24}$$

and reversal of time $t \to -t$. For further numerical studies we construct the Poincaré map T_ε of two-dimensional torus $\tau = (\xi, \eta) : 0 \le \xi < 2\pi, 0 \le \eta < 2\pi$ for period $t = 2\pi$, which is a diffeomorphism for $\varepsilon < 2$.

For sufficiently small ε, dynamics of T_ε is indistinguishable from the conservative ones see Fig. 12a,b. In particular, for the Poincaré map T_ε on an appropriately chosen cross-section elliptic islands are clearly observed, see Fig. 12b. Moreover, the time-averaged divergence of the vector field equals to zero up to the numerical accuracy. However, with the increase of ε the apparent conservativity gets destroyed; in particular, the average divergence starts differ from zero, the attractor of system no longer coincides with the repeller, see Fig. 13.

For the numerical evidence of the mixed dynamics at $\varepsilon > 0$ we do not search for the attracting/repelling periodic orbits directly (as their periods are apparently very large), as it was done e.g. in [29, 9*]. Instead, we establish their existence indirectly on the basis of numerical identification of the absolute Newhouse domains. In the paper [5*], we found non-transverse heteroclinic cycles which include saddles of small periods (up to period 7 in our experiments), see e.g. Figs. 14 and 15. Crucially, the saddles are non-conservative, i.e., one of the saddles is area-contracting (i.e. the Jacobian J of the period map is less than 1) and the other saddle is expanding ($J > 1$). It is proven in [34], [35] that bifurcations of such cycles that contain both contracting and expanding saddles lead to a simultaneous birth of infinitely many periodic attractors and repellers which have in the closure a non-empty intersection.

We find the pairs of non-conservative saddles by detecting local bifurcations of a peculiar type. We notice that the Poincare map T_ε in this model is the square of a certain orientation-reversing diffeomorphism $T_\star$ and find bifurcations which correspond to the emergence of a symmetric periodic point of $T_\star$ with the multipliers (+1,-1). This bifurcation is described by

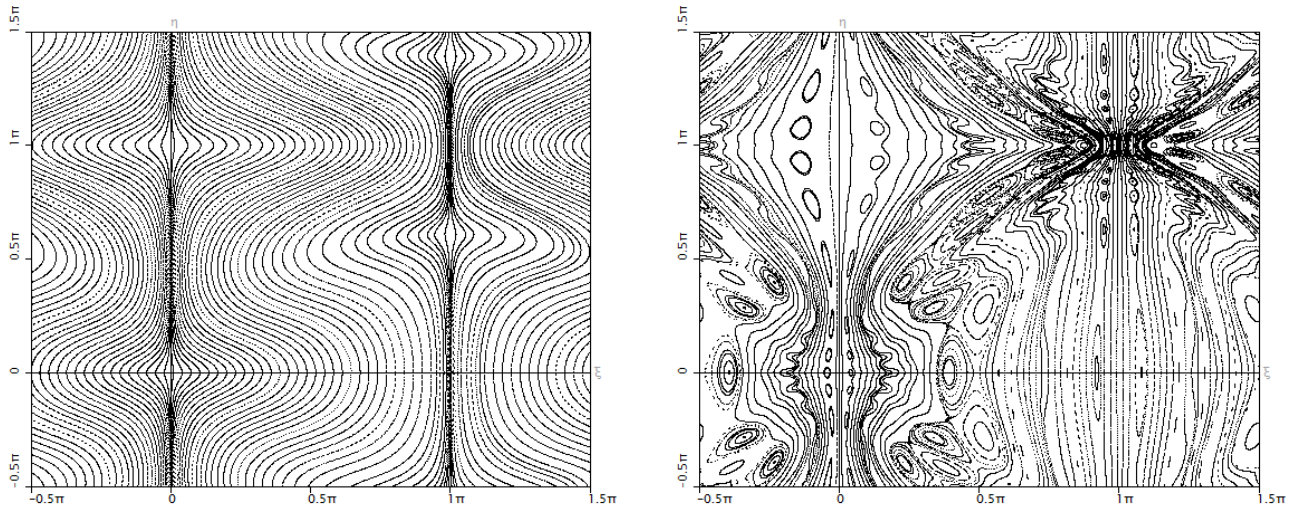

(a) (b)

Fig. 12: Phase portraits of the Poincaré map of system (23) with (a) $\varepsilon = 0.1$, and (b) $\varepsilon = 0.35$. The dynamics appears conservative.

the same normal form as the bifurcation of periodic points with multipliers (+1,+1) with an additional symmetry. Note that there are 4 different cases of normal forms for this bifurcation [36]. Two such cases have been detected in the Pikovsky-Topaj model (21).

The first case corresponds to the birth of one symmetric elliptic periodic orbit and a pair of saddles, one expanding and one contracting. These saddles are born along with heteroclinic connections, and the non-transverse intersections necessary for the proof of the mixed dynamics appear naturally (see Fig. 14).

The second case corresponds to the birth of one symmetric saddle periodic orbit, one sink, and one source. We find this bifurcation at $\varepsilon = \varepsilon_1^* \approx 0.6042$. Because of an additional symmetry, the Poincare map T_ε has simultaneously 2 fixed points which undergo this bifurcation. Thus, at $\varepsilon > \varepsilon_1^*$ the Poincare map T_ε has 8 fixed points: 2 sinks, 2 repellers, and 4 conservative saddles, see Fig. 15. Most of the orbits tend to the stable fixed points. However, at $\varepsilon < \varepsilon_1^{het} \approx 0.690$ there exist homoclinic intersections of the invariant manifolds of the saddle fixed points, see Fig. 15d (the moments of occurrence of heteroclinic and symmetric heteroclinic tangencies are shown in Fig. 15b,c). Therefore, the stable fixed points coexist with a chaotic set. Moreover, homoclinic tangencies can also exist for such ε. Despite the saddle fixed points here are conservative ($J = 1$), the conservativity of the Poincare map can be violated near the orbits of tangency and, according to [37], the reversible mixed dynamics can exist even for some interval of $\varepsilon > \varepsilon_1^*$, although it can be hard to detect.

At $\varepsilon < \varepsilon_1^*$ all the fixed points disappear, and we immediately see a large chaotic attractor and repeller, see Fig. 13. This phenomenon is related to the existence of homoclinic intersections of the separatrices of the fixed point at the bifurcation moment. Note that the numerically obtained attractor and repeller visibly intersect, which means that we have a large region in the phase space corresponding to the reversible mixed dynamics.

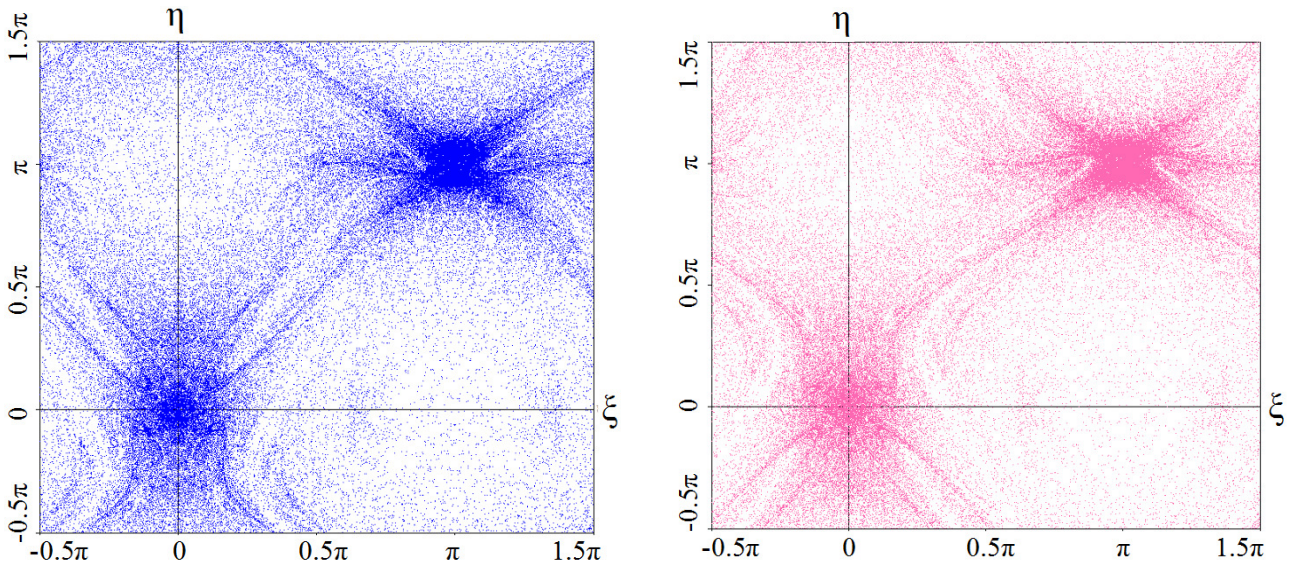

(a) Обратимый аттрактор (b) Обратимый репеллер

Fig. 13: Phase portraits of the Poincaré map of system (23) with $\varepsilon = 0.49$. (a) Forward iterations; the average divergence is $\overline{\text{div}} \approx -0.00122$) and (b) backward iterations $\overline{\text{div}} \approx 0.00122$. Note that the numerical attractor and repeller intersect but do not coincide.

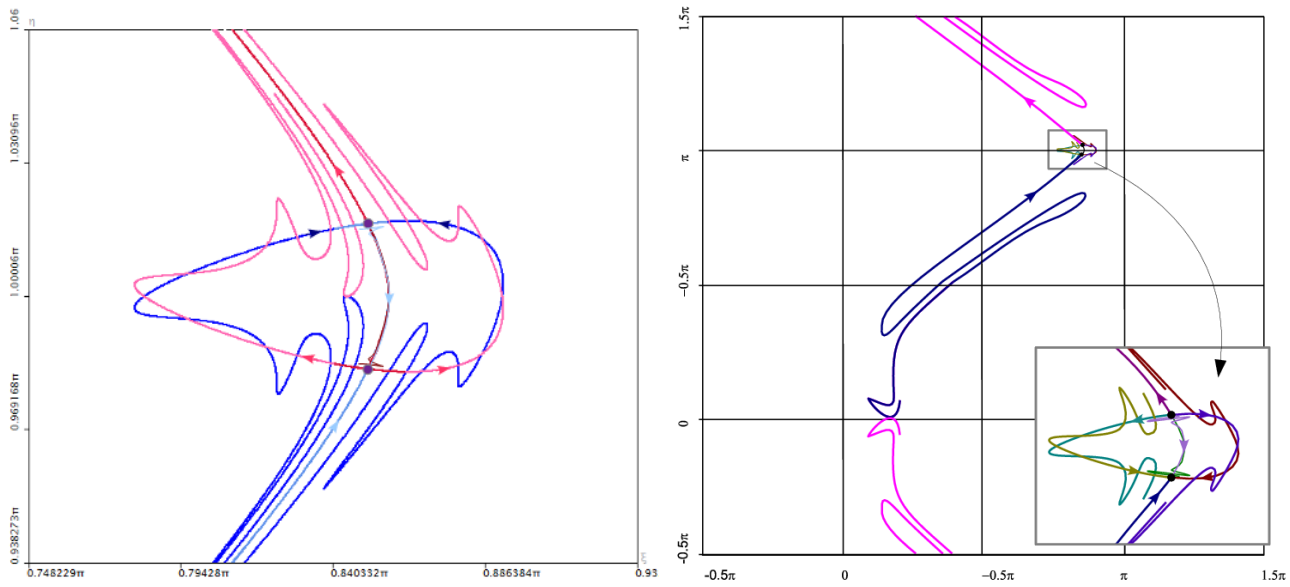

(a) (b)

Fig. 14: (a) Creating of "small" heteroclinic orbits at $\varepsilon \approx 0.46207$. (b) Creating of "large" heteroclinic orbits at $\varepsilon \approx 0.463$.

2.2.3 On the collision of chaotic attractor and chaotic repellers leading to the emergence of mixed dynamics.

An instant transition from dissipative chaos to mixed dynamics can be observed in reversible systems with small changes in parameter values (see e.g. the transition from Fig. 10c to Fig. 10b). In the paper [7*], an explanation of this phenomenon is proposed, and a scenario of the transition from conservative dynamics to mixed dynamics through the birth and then crisis of a strange attractor with a strange repeller is described.

Description of the scenario.

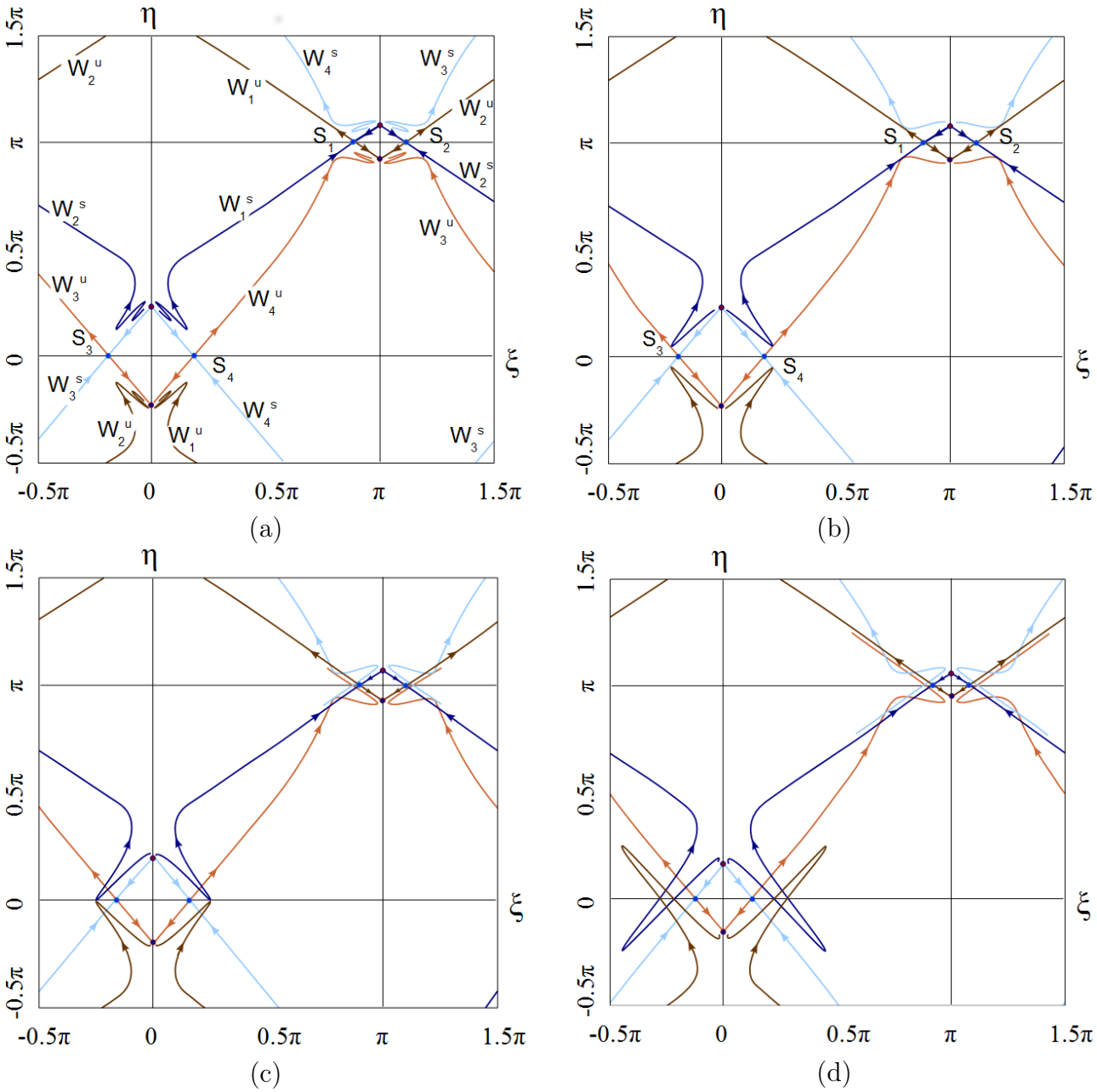

Fig. 15: The stable and unstable manifolds of saddle fixed points of T are shown. These manifolds (a) do not intersect, $\varepsilon = 0.7$, (b) form heteroclinic intersections, $\varepsilon = \varepsilon_1^{het} \approx 0.690$, and dynamics become chaotic. (c) Symmetric heteroclinic orbits appear at $\varepsilon = \varepsilon_2^{het} \approx 0.679$. (d) Developed homoclinic and heteroclinic tangles (shown at $\varepsilon = 0.650$) exist at $\varepsilon < \varepsilon_2^{het}$.

Let us consider a one-parameter family of two-dimensional reversible maps

$$\bar{x} = f(x, \varepsilon),$$

defined on a compact manifold and depending on a parameter ε. Suppose that for all ε these maps are reversible with respect to the same involution h (i.e. $f = h \circ f^{-1} \circ h$, where $h \circ h = id$) for which the set $Fix(h)$ of its fixed points (when $h(x) = x$) is one-dimensional.

Further, let O be a fixed point belonging to the line $Fix(h)$. Suppose that this point is elliptic for $\varepsilon < \varepsilon_0$ and it undergoes a reversible pitch-fork bifurcation [36] at $\varepsilon = \varepsilon_0$. After this, the point O becomes a saddle, and a symmetric pair of asymptotically stable, S^a, and completely

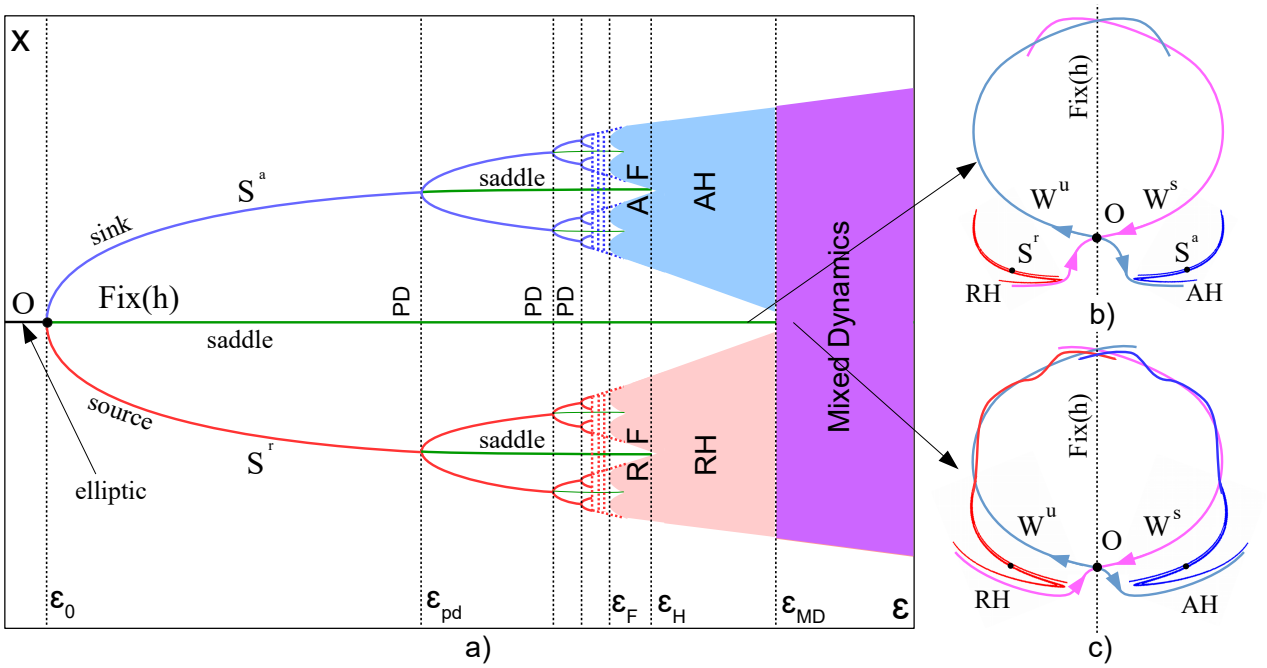

Fig. 16: The scenario of merger of a Hénon-like attractor with a Hénon-like repeller leading to the appearance of mixed dynamics in reversible two-dimensional maps.

unstable, S^r, fixed points (one point is symmetric to another with respect to h) appears near O (see Fig. 16, at $\varepsilon = \varepsilon_0$). We also suppose that, with further increase in the parameter, at $\varepsilon = \varepsilon_F$, a chaotic attractor AF is born via a cascade of period-doubling bifurcations with S^a. By the reversibility, a chaotic repeller RF is born from S^r at the same moment. We note, that after the first period-doubling bifurcation, points S^a and S^r become saddles.

Recall that immediately after the onset of chaotic dynamics through the cascade of period-doubling bifurcations, the chaotic attractor consists of disjoint components. With the further increase in ε these components merge pairwise (due to the occurrence of heteroclinic intersections between stable and unstable manifolds of the saddle orbits belonging to different components). Finally, two last components separated by the stable manifold of S^a are merged and the *homoclinic Hénon-like attractor* AH appears (see Fig. 16a at $\varepsilon = \varepsilon_H$ and Fig. 16b). By the reversibility, the homoclinic Hénon-like repeller RH containing the fixed point S^r occurs at the same moment.

With a further increase in ε, the Hénon-like attractor AH becomes larger and approaches the boundary of its basin of attraction which is formed by the stable manifold W^s of the saddle fixed point O (accordingly, the basin for RH is bounded by the unstable manifold W^u of the same point O). Also we note that both stable and unstable manifolds are separated by the point O into pairs of stable and unstable separatrices, and one pair of separatrices already intersects, while another does not, see Fig. 16b.

When $\varepsilon = \varepsilon_{MD}$, the crisis of attractor AH and repeller RH occurs (AH collides with the boundary of its absorbing domain W^s, while RH symmetrically collides with the boundary of its repulsing domain W^u), after which both these sets get involved into the same homoclinic structure, the attractor merges with the repeller, mixed dynamics appear, see Fig. 16c.

Implementation of the scenario on the example of nonholonomic model of

Suslov top.

In the paper [7*] it is shown that the described above scenario is implemented in the nonholonomic model of Suslov top (19). Let us fix the parameters in this model, as described in the Sec. 2.2.1, and carry out a one-parameter analysis considering I_{23} as a control parameter.

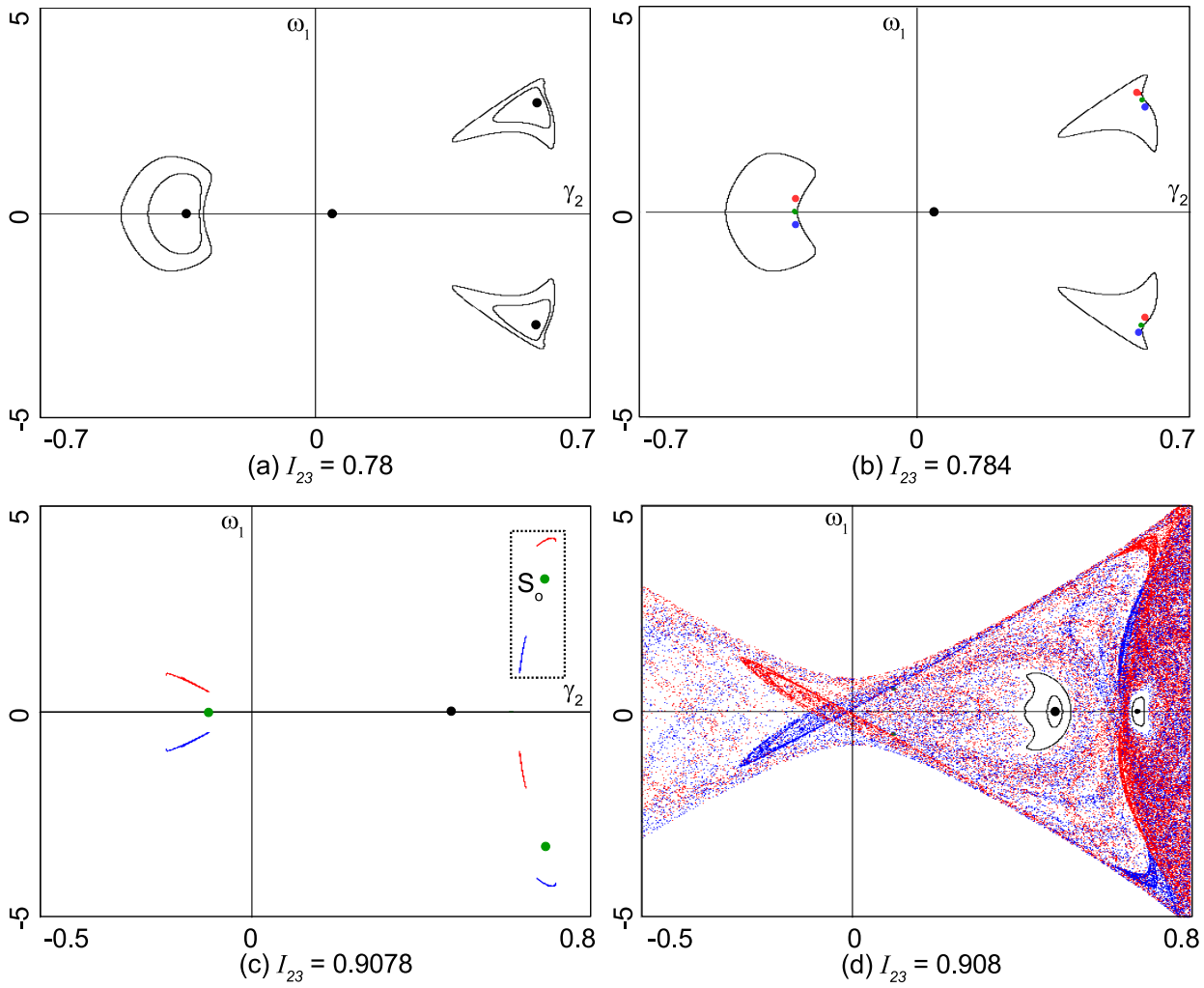

Fig. 17: Scenario of the emergence of mixed dynamics in the nonholonomic model of Suslov top (19).

At $I_{23} = 0.692$, a symmetric elliptic point of period 3 (S_o) appears in the system, see Fig. 17a. Then, at $I_{23} = 0.7835$, this point undergoes a symmetry-breaking bifurcation. After this, S_o becomes of a saddle type and the asymptotically stable and completely unstable points of period 3 appear in its neighborhood, see Fig. 17b. With the further increase in the parameter I_{23}, the Hénon-like attractor and Hénon-like repeller appear from the stable periodic point and the completely unstable point, respectively, see Fig. 17c.

It is worth noting that the system under consideration is monostable in the considered parameter range, i.e., the Hénon-like attractor and the Hénon-like repeller are global attractor and repeller in the system. Then, at $I_{23} = 0.9079$, the attractor collides with the repeller disappear according to the scenario described above. The attractor, which appears after that, intersects with the repeller, and mixed dynamics appear, see Fig. 17d.

Let us describe in more detail the homoclinic bifurcations leading to the appearance of

mixed dynamics in the system under consideration. Figure 18 shows the location of the stable W_o^s and unstable W_o^u separatrices of the symmetric saddle point S_o, as well as the unstable separatrix W_a^u, which forms the Hénon-like attractor, and the stable separatrix W_r^s which forms the Hénon-like repeller. At $I_{23} < 0.9079$, the stable separatrix W_0^s forms the boundary of absorbing domain for the Hénon-like attractor, while the unstable separatrix W_0^u forms the boundary of repulsion domain for the Hénon-like repeller, see Fig. 18a. At $I_{23} > 0.9079$, the unstable manifold W_a^u, which forms the attractor, intersects with the separatrix W_o^s, whereas the manifold W_r^s, which forms the repeller, intersects with W_o^u. In this case, since the second pair of the separatrices of the saddle point S_0 already intersects transversally (which is not shown in the figure for convenience), intersection between the separatrices W_a^u and W_r^s appears immediately, see Fig. 18b. Therefore, the attractor arising after the crisis of the Hénon-like attractor intersects with the repeller, and mixed dynamics manifest itself, see Fig. 18b.

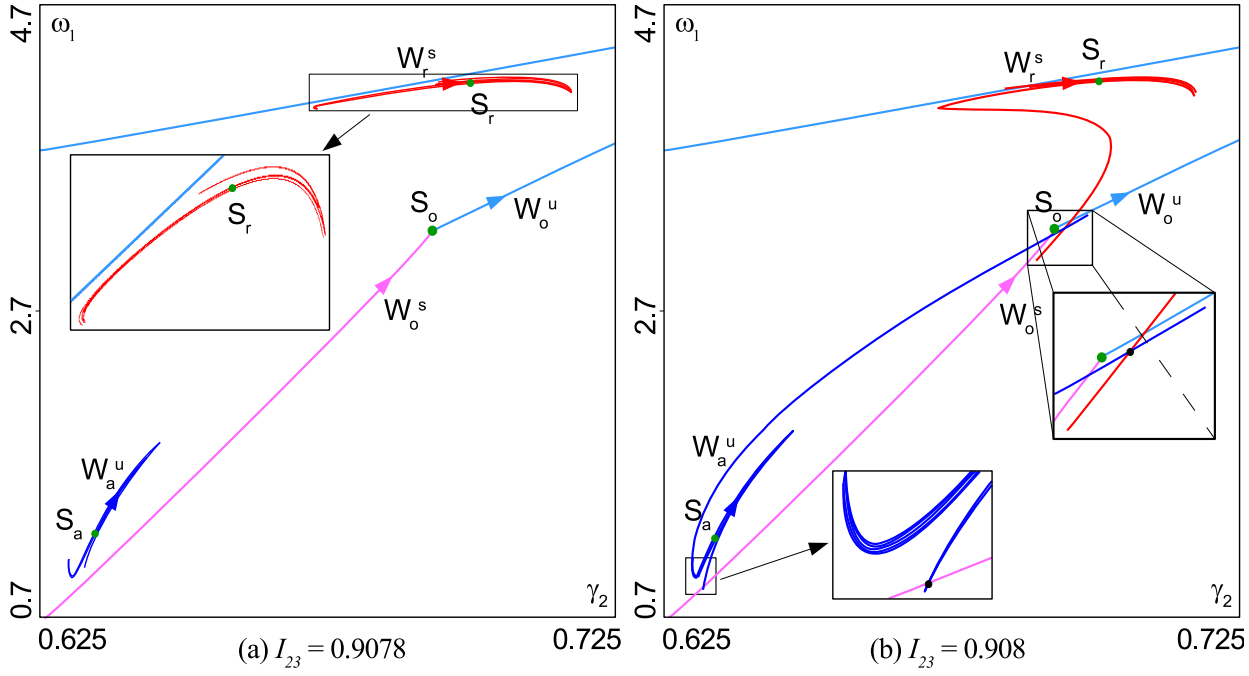

Fig. 18: Homoclinic bifurcations leading to the appearance of the mixed dynamics: (a) $I_{23} = 0.9078$, (b) $I_{23} = 0.9080$.

2.2.4 Strongly dissipative mixed dynamics.

In the nonholonomic model of Suslov top, as well as in other known reversible models with mixed dynamics, the difference between the numerically obtained chaotic attractor and chaotic repeller decreases with increasing computation time (however, the asymmetry in the distribution of points in the attractor and repeller remains). This result is in good agreement with Theorem 2 from [28], which states that for any system if a chain-transitive attractor intersects with a chain-transitive repeller, then these two sets must coincide. In our case, the attractor (repeller) is a quasiattractor (quasirepeller) according to Afraimovich and Shilnikov. In this case, e.g., the attractor contains a large chain-transitive nonuniformly hyperbolic set with very small holes, inside which there are stable trajectories of large periods, which are

usually elusive in numerical experiments.[3]

In the paper [8*], on the example of system governing dynamics of two-point vortices perturbed by an acoustic wave, we present a far from conservative example of reversible mixed dynamics, when a strange attractor and a strange repeller have a non-empty intersection but are very much different from each other, and this difference does not seem to vanish with a reasonable increase in the computation time, in an apparent contradiction with the above mentioned theorem from Ref. [28], see Fig. 19b.

As in the nonholonomic model of Suslov top, this type of mixed dynamics arises as a result of the collision of a Hénon-like attractor with a Hénon-like repeller, see Fig. 19a.

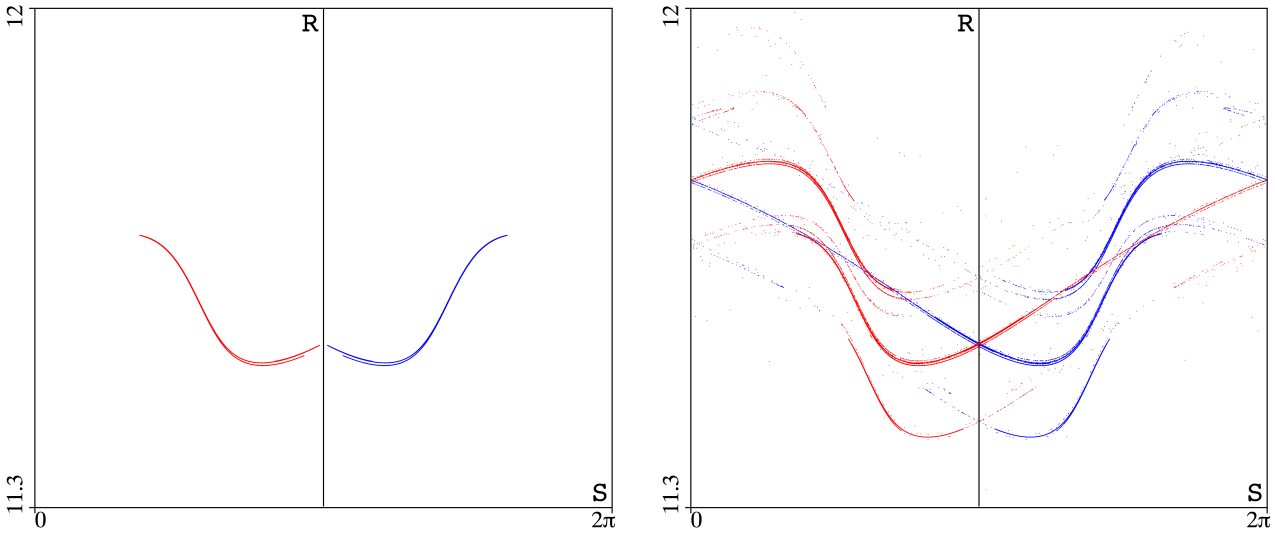

Fig. 19: The phase portraits of the attractor (in blue) and the repeller (in red) in the Poincaré map for the model of two point vortices perturbed by an acoustic wave. (a) The Hénon-like attractor is separated from the Hénon-like repeller. (b) Mixed dynamics after the collision of the Hénon-like attractors with the Hénon-like repellers.

We call such phenomenon the *strongly dissipative mixed dynamics*. In comparison with the previously known cases of mixed dynamics, the phase volume contraction rate (the sum of Lyapunov exponents) on the attractor for strongly dissipative mixed dynamics is much less than zero, which makes the system far from conservative and, in our opinion, makes the large difference between the distribution of points in the attractor and the repeller possible.[4] We believe that the computation time needed to see that the intersecting attractor and repeller occupy the same region in the phase space, as prescribed by [28], is extremely large in this case and is unachievable in realistic simulations.

In the paper [8*] we also describe a bifurcation scenario for the transition from conservative to mixed dynamics in the studied vortex model. The main part of this scenario is the collision of the Hénon-like attractor with the Hénon-like repeller, which occurs due to the appearance

[3]For example, in the paper [38], it is shown that the Hénon attractor can contain a "hole" of diameter 10^{-51}, in which a stable trajectory of period 115 lies. In standard numerical calculation (with double precision numbers), such effects cannot be observed.

[4]As we now understand, this is due to a very strong asymmetry of singular invariant measures concentrated on the attractor and repeller, which is formalized by the fact that the so-called Kantorovich-Rubinstein-Wasserstein distance between the attractor and the repeller becomes very large as the dissipation [39] increases.

of heteroclinic cycles between the invariant manifolds of a pair of saddle fixed points, one of which belongs to the attractor, and the other belongs to the repeller, see Sec. 2.2.3.

2.2.5 Mixed dynamics in the nonholonomic model of rubber disk on a plane.

In the paper [9*], with help of the concept of mixed dynamics, it was established that there is no smooth invariant measure in the nonholonomic model of rubber disk on a plane.

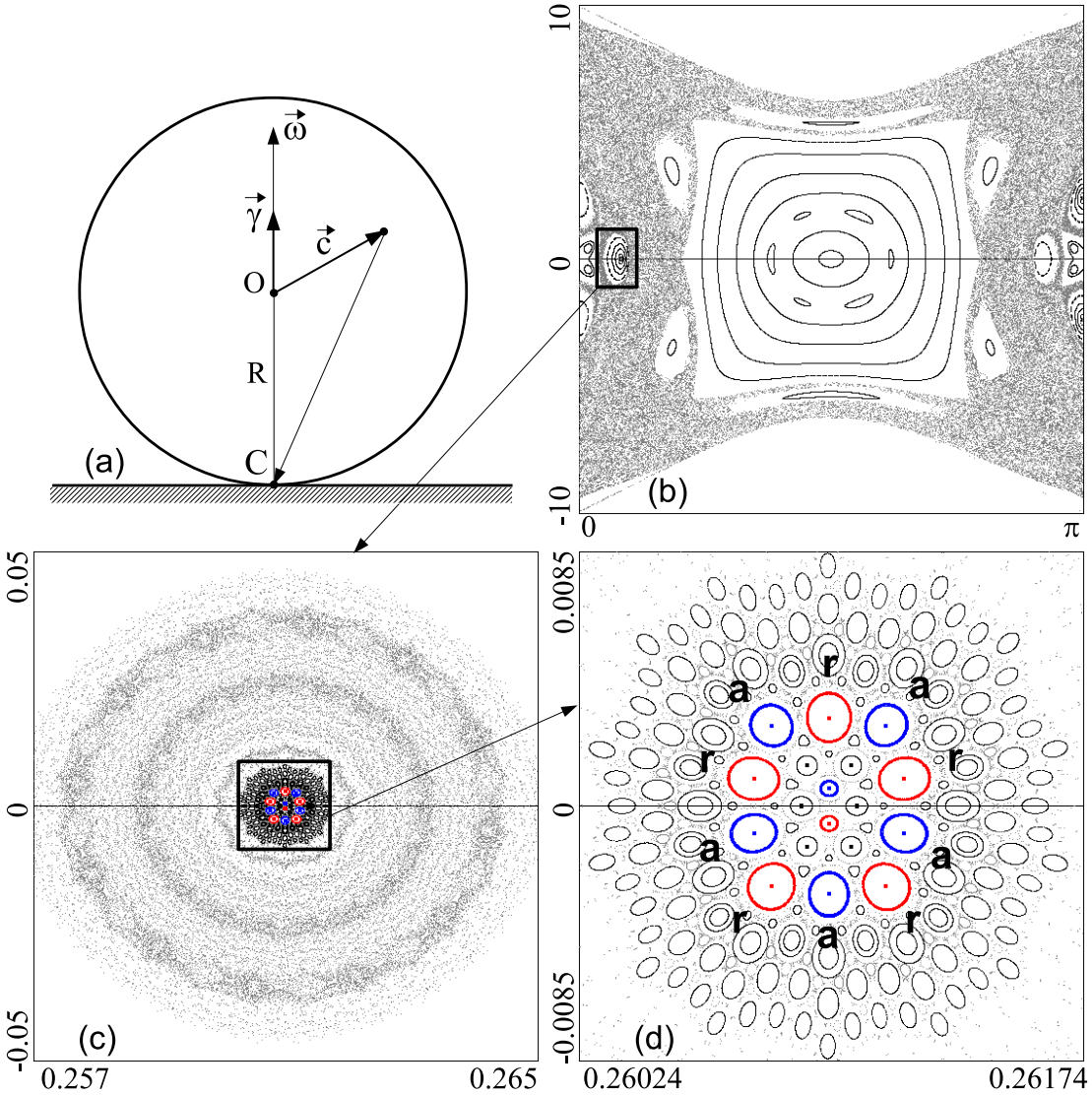

Fig. 20: Dynamics of the rubber disc on a phase plane (θ, p_θ), where θ is the deflection angle of the disc from the vertical axis and p_θ is its generalized momentum: (a) scheme of the disc; (b) phase portrait in the Poincaré map; (c) and (d) its enlarged fragments (with 1000× magnification from (b) to (d)). In the phase portrait of part (d), attractors (a), repellers (r), and their absorbing/repulsing domains are marked (the thick circles around the attractors/repellers are actually pieces of extremely weakly twisting spirals).

The vortex model and the nonholonomic model of Suslov top considered above exhibit mixed dynamics for which the full attractor of the system is clearly different from its full repeller. However, in some nonholonomic systems, such a difference is hardly noticeable. It can be only detected under careful investigation of the phase portrait of the system, after a preliminary study of bifurcations of emergence of stable periodic orbits.

Among the models of this type, there is a nonholonomic model of rubber disk – a balanced round solid body of zero thickness – that has different principal moments of inertia [40, 41, 42], see Fig. 20a. The motion of such a disk along the plane is subject to a pair of nonholonomic constraints: one forbids slipping (the velocity at the point of contact is zero), while the other prevents spinning around the vertical axis. Thus, as in the case of Suslov top, the dynamics of the rubber disk on a plane is described by a three-dimensional flow or a two-dimensional Poincaré map.

In numerical simulations, the behavior of the orbits in this map is very similar, even in small details, to the conservative one (see, e.g., Fig. 20b). Therefore, the question of the existence of a smooth invariant measure naturally arises for this model. However, instead of searching for an invariant measure, it is reasonable first to answer another, even more natural, question about the existence of mixed dynamics. This question has been answered in the affirmative. Inside the seemingly conservative chaos, on small scales (on the order of $10^{-3} \times 10^{-3}$)), it is possible to detect coexisting elliptic, asymptotically stable, and completely unstable periodic points located inside zones with chaotic behavior of orbits (Figs. 20c and 20d). Thus, the approach to studying the model from the point of view of the concept of mixed dynamics turned out to be very successful in this case as well.

2.3 A software package for the study of chaos in multidimensional dynamical systems.

The numerical methods for studying multidimensional dynamical systems developed by the author of this thesis are implemented in the form of ready-made software solution "Computer Dynamics: Chaos", presented in three versions 5.0, 5.5, and 6.0. Versions 5.0 and 5.5 was patented by the group of authors, which includes the dissertation applicant [13*, 14*].

The software package can be used for the study of a wide class of dynamical systems described by both systems of ordinary differential equations and discrete maps. A flexible system of settings for methods and tools allows one to select parameters that are optimal for research, ensuring a balance between the accuracy of results and the time of their obtaining.

The implemented toolkit of the software package allows:

- to identify in the parameter space regions with conservative, dissipative, and mixed chaos;
- to check the pseudohyperbolicity of strange attractors;
- to build diagrams of homoclinic bifurcations;
- to identify in the parameter space regions with "wild" behavior;
- to implement new models using the developed interface for creating custom problems.

The software package is implemented using C++ language. To speed up time-consuming computations associated with a two-parameter analysis, most of the methods are implemented with help of parallel programming technologies using both the cores of the central and graphics processor units (CPU and GPU). Parallelization for the GPU is carried out using CUDA technology.

To run calculations in the package, one should:

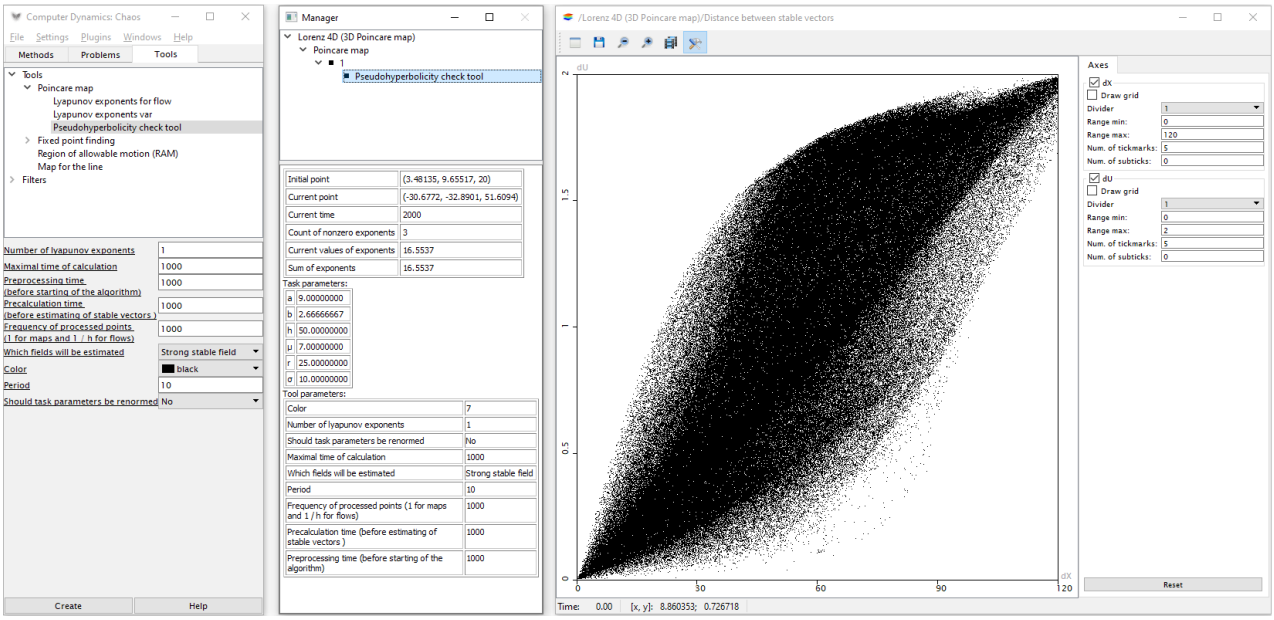

Fig. 21: Screenshot of the software package "Computer Dynamics: Chaos" when building the continuity diagram for the subspace E^{ss} in the four-dimensional Lorenz model: (a) main control window; (b) window with the results of the pseudohyperbolicity verification; (c) the E^{ss}-continuity diagram, confirming the pseudohyperbolicity of the wild spiral attractor.

- to select a task from the Problems list and to set the corresponding control parameters;
- to select an integration method from the Methods list (if the problem under study is described by a system of differential equations) and to set the method parameters (initial step, maximum step, relative and absolute errors – for methods with variable steps);
- to select a research tool from the Tools list and to set its settings via the corresponding menu.

Then, one can run the calculations. The results of the work are exported to a file, and also displayed in the window of selected tool. Figure 21 shows a screenshot of the working software package when checking the wild spiral attractor for pseudohyperbolicity, see Section 2.1.2.

The developed software package is equipped with a module for creating user systems. After creating a new system, it appears in the general Problem list and the same integration methods and research tools can be applied for its study as for other systems.

References

[1] Anosov D.V., Aranson S.K., Grines V.Z., Plykin R.V., Sataev E.A., Safonov A.V., Solodov V.V., Starkov A.N., Stepin A.M., Shlyachkov S.V. *Dynamical systems with hyperbolic behavior* //Itogi Nauki i Tekhniki. Seriya "Sovremennye Problemy Matematiki. Fundamentalńye Napravleniya". M.: VINITI, 66, 1991, pp. 5–242.

[2] Lorenz E.N. *Deterministic nonperiodic flow* //Journal of atmospheric sciences, **20(2)** (1963), pp. 130–141.

[3] Afraimovich V.S., Bykov V.V., Shilnikov L.P. On the origin and structure of the Lorenz attractor //In Akademiia Nauk SSSR Doklady, **234** (1977), pp. 336–339.

[4] Afraimovich V.S., Bykov V.V., Shilnikov L.P. *Attractive nonrough limit sets of Lorenz-attractor type* //Trudy Moskovskoe Matematicheskoe Obshchestvo, **44** (1982), pp. 150–212.

[5] Turaev D.V., Shilnikov L.P. *An example of a wild strange attractor* //Sbornik: Mathematics, **189(2)** (1998), p. 291.

[6] Afraimovich, V.S. and Shilnikov, L.P. *Strange attractors and quasiattractors* //Strange attractors and quasiattractorsNonlinear Dynamics and Turbulenceed (G.I. Barenblatt, G. Iooss and D.D. Joseph (Boston, MA: Pitmen)) 1983.

[7] Kuptsov P.V., Kuznetsov S.P. *Lyapunov analysis of strange pseudohyperbolic attractors: angles between tangent subspaces, local volume expansion and contraction* //Regular and Chaotic Dynamics, **23(7)** (2018), pp. 908–932.

[8] Galias Z., Tucker W. *Is the Henon attractor chaotic?* //International Journal of Bifurcation and Chaos, **25(3)** (2015), 033102.

[9] Shilnikov A.L., Shilnikov L.P., Turaev D.V. *Normal forms and Lorenz attractors* //International Journal of Bifurcation and Chaos, **3(05)** (1993), pp. 1123–1139.

[10] Newhouse S.E. *The abundance of wild hyperbolic sets and non-smooth stable sets for diffeomorphisms* //Publications Mathématiques de l'IHÉS, **50** (1979), pp. 101-151.

[11] Gonchenko S.V., Ovsyannikov I.I., Simó C. and Turaev D. 2005 *Three-dimensional Hénon-like maps and wild Lorenz-like attractors* //International Journal of Bifurcation and Chaos, **15(11)** (2005), 3493-3508.

[12] Shilnikov A.L. *Bifurcation and chaos in the Morioka-Shimizu system* Methods of Qualitative Theory of Differential Equations (Gorky University Press), 1986, pp. 180-93.

[13] Shilnikov A.L. *On bifurcations of the Lorenz attractor in the Shimizu–Morioka model* //Physica D: Nonlinear Phenomena, **62(1-4)** (1993), pp. 338–346.

[14] Tucker W. *The Lorenz attractor exists* //Comptes Rendus de l'Académie des Sciences-Series I-Mathematics, **328.12** (1999), pp. 1197-1202.

[15] Turaev D.V., Shilnikov L.P. *Pseudohyperbolicity and the problem on periodic perturbations of Lorenz-type attractors* //Doklady Mathematics, **418(1)** (2008), pp. 17–21.

[16] Gonchenko S., Karatetskaia E., Kazakov A., Safonov K., Turaev D. *On new discrete attractors of Lorenz type in orientation reversing three-dimensional Hénon Maps and the bifurcation (-1, i, -i)* (в работе), 2022.

[17] Gonchenko A.S., Gonchenko S.V.., Shilnikov L.P. *Towards scenarios of chaos appearance in three-dimensional maps* //Rus. J. Nonlin. Dyn, **8(1)** (2012), C. 3-28.

[18] Borisov A.V., Mamaev I.S *Rigid Body Dynamics: Hamiltonian Methods, Integrability, Chaos.* – Research and Publishing Center "Regular and Chaotic Dynamics" (2005).

[19] Guckenheimer J. *A strange, strange attractor* The Hopf Bifurcation Theorem and its Applications (Berlin: Springer) (1976), pp. 368–81.

[20] Guckenheimer J., Williams R.F. *Structural stability of Lorenz attractors* Inst. Hautes Etudes Sci. Publ. Math. **50** (1979), pp. 59–72.

[21] Shilnikov L.P. *The bifurcation theory and quasi-hyperbolic attractors* //Uspehi Mat. Nauk, **36** (1981), pp. 240–241.

[22] Capiński M.J, Turaev D., Zgliczyński P.*Computer assisted proof of the existence of the Lorenz attractor in the Shimizu–Morioka system* //Nonlinearity, **31(12)** (2018), pp. 5410.

[23] Lyubimov D.V., Zaks M.A. *Two mechanisms of the transition to chaos in finite-dimensional models of convection* //Physica D: Nonlinear Phenomena, **9(1-2)** (1983), pp. 52–64.

[24] Chua L.O., Shilnikov L.P., Shilnikov A.L., Turaev D.V. *Methods Of Qualitative Theory In Nonlinear Dynamics (Part Ii).* **5** World Scientific, 2001.

[25] Rovella A. *The dynamics of perturbations of the contracting Lorenz attractor* //Boletim da Sociedade Brasileira de Matemática-Bulletin/Brazilian Mathematical Society, **24(2)** (1993), pp. 233-259.

[26] Morales C. A., Pacifico M. J., Martin B. S. *Contracting Lorenz attractors through resonant double homoclinic loops* //SIAM journal on mathematical analysis, **38(1)** (2006), pp. 309-332.

[27] Gonchenko A. S., Gonchenko S. V. *Variety of strange pseudohyperbolic attractors in three-dimensional generalized Hénon maps* //Physica D: Nonlinear Phenomena, **337** (2016), pp. 43-57.

[28] Gonchenko S.V., Turaev D.V. *On three types of dynamics and the notion of attractor* //Proceedings of the Steklov Institute of Mathematics **297** (2017), pp. 116–137.

[29] Kazakov A. O. *Strange attractors and mixed dynamics in the problem of an unbalanced rubber ball rolling on a plane* //Regular and Chaotic Dynamics, **18(5)** (2013), pp. 508-520.

[30] Gonchenko A. S., Gonchenko S. V., Kazakov A. O. *Richness of chaotic dynamics in nonholonomic models of a Celtic stone* //Regular and Chaotic Dynamics, **18(5)** (2013), pp. 521-538.

[31] Kozlov V.V. *On the theory of integration of the equations of nonholonomic mechanics*, **8(3)** (1985), pp. 85–101.

[32] Benettin G., Galgani L., Giorgilli A., Strelcyn J.-M. *Lyapunov characteristic exponents for smooth dynamical systems and for Hamiltonian systems; a method for computing all of them. Part 1: Theory* //Meccanica, **15(1)** (1980), pp. 9-20.

[33] Pikovsky A., Topaj D., *Reversibility vs. synchronization in oscillator latties*, Physica D: Nonlinear Phenomena, **170** (2002), pp. 118-130.

[34] Gonchenko S.V., Shilnikov L.P., Turaev D.V. *On Newhouse domains of two-dimensional diffeomorphisms which are close to a diffeomorphism with a structurally unstable heteroclinic cycle* //In Proc. Steklov Inst. Math, **216** (1997), pp. 70-118.

[35] Lamb J. S. W., Stenkin O. V. *Newhouse regions for reversible systems with infinitely many stable, unstable and elliptic periodic orbits* //Nonlinearity, **17(4)** (2004), pp. 1217.

[36] Lerman L.M., Turaev D.V. *Breakdown of Symmetry in Reversible Systems* //Regul. Chaotic Dyn., **17(3-4)** (2012), pp. 318-336.

[37] Delshams A., Gonchenko S. V., Gonchenko V. S., Lazaro J. T., Stenkin, O. *Abundance of attracting, repelling and elliptic periodic orbits in two-dimensional reversible maps* //Nonlinearity, **26(1)** (2012), pp. 1.

[38] Galias Z., Tucker W. *Is the Hénon attractor chaotic?* // Chaos: An Interdisciplinary Journal of Nonlinear Science, **25(3)** (2015), p. 033102.

[39] Chigarev V., Kazakov A., Pikovsky A., *Kantorovich–Rubinstein–Wasserstein distance between overlapping attractor and repeller* // Chaos: An Interdisciplinary Journal of Nonlinear Science, **30(7)** (2020), p. 073114.

[40] Kozlov V.V., Afonin A.A. *The fall problem for a disk moving on a horizontal plane* //Rossijskaya Akademiya Nauk, Izvestiya, Mekhanika Tverdogo Tela, **1** (1997) pp. 7–13.

[41] Kozlov V. V. *Several Problems on Dynamical Systems and Mechanics* //Nonlinearity, **21(9)** (2008), pp. 149–155.

[42] Bizyaev I. A., Borisov A. V., Mamaev I. S.. *An Invariant Measure and the Probability of a Fall in the Problem of an Inhomogeneous Disk Rolling on a Plane* // Regular and Chaotic Dynamics, **23(6)** (2018), pp. 665–684.